July 2020

CONTRIBUTION OF VELOCITY CONGRUENCY AND APPARENT STIFFNESS TO INTERFERENCE OF BIMANUAL RHYTHMIC-DISCRETE MOVEMENTS.

Marcelline E. Dechenaud
Louisiana State University and Agricultural and Mechanical College

CONTRIBUTION OF VELOCITY CONGRUENCY AND APPARENT STIFFNESS TO INTERFERENCE OF BIMANUAL RHYTHMIC-DISCRETE MOVEMENTS.

A Thesis

Submitted to the Graduate Faculty of the
Louisiana State University and
Agricultural and Mechanical College
in partial fulfillment of the
requirements for the degree of
Master of Science

in

The Department of Kinesiology

by
Marcelline, Eugénie, Dechenaud
M.S., Université Claude Bernard Lyon I, 2017
August 2020

On n'est pas à l'abri que ça marche.

—Gérard J. E. Dechenaud

Table of Contents

List of Tables

List of Figures

Abstract

Many actions feature rhythmic and discrete movements, individually or in combinations. Rhythmic movements are defined as those having no clearly defined start and endpoint, while discrete movements have a definite starting and ending posture. Performing a discrete movement against a base rhythm by the contralateral limb typically speeds up the rhythmic movement – indicating the presence of bimanual coupling. While bimanual rhythmic/rhythmic interaction has been studied extensively in the field [2], understanding of the interaction between discrete and rhythmic movements has been less represented. In this thesis, I examined two potential sources of interlimb interference during rhythmic-discrete bimanual actions: 1) velocity congruence of the limbs, 2) co-contraction level of the synergist muscles. Hypothesis 1 predicted that the extent of rhythmic-discrete interference depends on the discrepancy between the velocities of the rhythmic and discrete movements, such that faster discrete movement would speed up the rhythmic movement and vice versa. Hypothesis 2 predicted that speeding up the rhythmic movement following the discrete response would be associated with increased muscle co-contraction in the rhythmic limb because higher apparent stiffness typically increases the natural frequency of oscillations. To address these hypotheses, I used a computational model of upper limb movements proposed by Ronsee et al. [1] that allows simulation of both unimanual and bimanual rhythmic and discrete movements using the central pattern generator (CPG) concept. Discrete movement with an amplitude of 60 deg was simulated in two velocity conditions: Slow (peak velocity: 163 deg/s) and Fast (249 deg/s), these values differed by approximately 20% from the peak velocity of the rhythmic movement. Phase discrete movement initiation within rhythm was also manipulated. Dependent measures included

rhythmic movement period, amplitude, phase, and level of co-contraction following the initiation of the discrete response were examined. The results showed that 1) the velocity of the discrete movement does not account for the changes of rhythmic behavior and (2) the level of co-contraction and the period shift of the rhythmic arm do not co-vary. However, the results suggested that the response of the rhythmic arm is dependent of the rhythmic movement's phase during which the discrete movement is initiated.

Chapter 1. Introduction

1.1. Bimanual activities

Bimanual coordination of movements refers to actions that are performed by two hands simultaneously to achieve a single behavioral goal [3]. Many daily activities require such coordination: one can pour a glass of water while holding the bottle in one hand and the glass in the other, type on a keyboard with both hands, or play a musical instrument such as guitar. For all those movements, the degree of collaboration and interference between the two hands depends on the required spatial and temporal constraints [4]. Temporal constraints are constraints given to the task performer about the timing during which the task has to be performed whereas spatial constraints give to the performer constraints on the space within which the task has to be performed. Previous studies are largely assessing the effect of those constraints on bimanual rhythmic/rhythmic tasks or bimanual discrete/discrete tasks, but lesser attention has been brought to very common bimanual rhythmic/discrete tasks of the human movement repertoire [4].

Discrete and rhythmic movements have been defined by Hogan and Sternad [5]. They proposed a more precise mathematical definitions of kinematic features of rhythmic and discrete movements suggesting that a rhythmic movement consists of a periodic movement and can be identified thanks to the regularity of its periodicity, and a discrete movement is defined by the pauses of the end-effector between each movement. Those two types of movement have been hypothesized to be two basic movement types in the literature [6, 7, 8, 9, 10, 11, 12]. Three different points of view regarding those definitions can be highlighted. The first point of view states that discrete movements are the fundamen-

tal movement type, and rhythmic movements are a succession of discrete movements. The second point of view defends the opposite, i.e. the rhythmic movement is fundamental, and discrete movements are truncated rhythms. The last point of view states that rhythmic and discrete movements are two independent classes of movement generated by different neural control schemes. This latter hypothesis has been strengthened by Ikegami [6] and Howard [13, 8], both showing strong transfer of acquired skills [14] from discrete to rhythmic, but incomplete transfer from rhythmic to discrete movements.

When performing rhythmic bimanual movements, a robust spatiotemporal coupling is exhibited when the movements are produced at a common frequency, showing a preference for the in-phase and anti-phase stable relationships [15, 16]. When considering coupling between rhythmic-discrete bimanual movements, Wei et al. [17] tested healthy individuals on the initiation of rhythmic and discrete movements from the contralateral hand to hand performing the base rhythmic movement. They found that a rhythmic contralateral movement is more likely to be initiated in-phase with the base rhythmic movement, but a discrete contralateral movement could be initiated independently to the phase of the base rhythmic movement, i.e. the reaction time of the initiation of a discrete movement is independent of the phase of the rhythmic movement, in contrary to the rhythmic one. Those results indicate a stronger bimanual coupling of rhythmic-rhythmic movements compared to discrete-rhythmic movements. Nevertheless, the base rhythmic movement typically shows a phase reset after the initiation of the discrete movement. Phase reset refers to the deviation of the rhythmic movement phase due to the discrete movement. Frequently, phase reset is a phase advance – i.e., the period of the rhythm is faster after the discrete response than before, indicating that contralateral discrete movements are not

performed completely independently from the rhythmic ones [18].

Multiple reasons might be at the origin of the phase reset observed in the base rhythmic movement when the perturbation (i.e. the discrete movement) occurs. The first reason leading to the phase reset of the fundamental rhythmic pattern might be temporal assimilation [19, 20] depending on which one prefers to initiate bimanual movements at the same time. For example, if one tries to simultaneously reach for a cup of coffee and a spoon using two hands, both will likely start the movement at about the same time. Such two-hands coordinative coupling findings have also been discussed by Kelso et al. [19] who showed the almost perfect synchrony of peak velocity and acceleration between the two hands during the synchronous bimanual movement triggered by a 'go' signal. The second reason leading to the phase reset of the rhythmic movement might be muscle co-contraction. In cases where unpredictable perturbations happen, human subjects are attempting to control their movements by increasing the apparent joint stiffness [21] by increasing the level of muscle co-contraction [22]. The third factor that might account for the phase reset of the rhythmic movement while dual-tasking is the attentional focus [17] which is deflected from the rhythmic movement when the contralateral one occurs, causing a disruption in the original motor command. The last factor that may cause interference between the two different movement types is the neuronal cross-talk [23, 24]. Neural crosstalk is a "mirror" image command sent to the homologous muscle of the contralateral limb [23, 25]. Movement patterns known as anti-phase or asymmetrical require the activation of non-homologous muscles whereas in-phase or symmetrical movements patterns require the activation of homologous patterns [26, 20]. It is widely shown in the literature that bimanual frequency relationships other than 1:1 or 2:1 are difficult to perform with-

out practice [3, 20, 27, 28, 29]. Then, when asymmetric muscle contraction is required by a rhythmic-discrete asynchronous bimanual task, an interference produced by neural cross-talk occurs [30]. Previous work by Calvin et al. [4] investigated the interference of bimanual rhythmic and discrete movements performed at the wrist joint. Their findings suggest that the rhythmic movement can be accelerated or decelerated depending on the timing of execution of the discrete movements. To the best of our knowledge, it remains unclear under which conditions of the discrete movement the rhythmic limb increases or decreases the speed of its movement upon perturbation.

1.2. Goals of the study and hypotheses

The goal of this thesis is to evaluate the contribution of temporal assimilation effects and muscle co-contraction levels to the degree of interference between bimanual discrete-rhythmic movements. Hypothesis 1 is that the extent of rhythmic-discrete interference will depend on the discrepancy between the velocities of the rhythmic and discrete movements. I predict that the rhythmic movements will slow down (increase period) in response to the discrete movement performed at a slower velocity than the base rhythmic movement. At the same time, rhythmic movements will speed up (decrease period) after the discrete movements that are faster than the velocity of the base rhythmic movement occur. This hypothesis will be tested using the simulated data from a computational model of rhythmic-discrete coordination proposed by Ronsse et al. [1]. Model predictions for interference stemming from discrete movements of varying velocities will be compared with the observed interference patterns. In addition, the contribution of apparent joint stiffness to the rhythmic movement interference will be assessed. Previous studies have

suggested that speeding up the rhythmic movement following the discrete response may stem from an increase in the apparent stiffness of the joint performing the rhythmic movement [17], but this has not been tested directly using metrics of muscle co-contraction based on surface electromyography to the best of our knowledge. Hypothesis 2 is that those individuals who show decreased movement period (i.e. speed up) following the discrete response should also show increased levels of muscle co-contraction. The current study is a modelling work so that both hypothesis stated above will be tested using a computational model developed by Ronsse et al. [1]. The computational model used uses a Central Pattern Generator structure that will be further described in this document.

1.3. Central Pattern Generator (CPG)

Early in motor behavior research, interests have been oriented toward discovering the origin and usages of the two class movements previously introduced: discrete and rhythmic movements. Although discrete movements have mostly been observed in recent species with developed upper-extremities, rhythmic movements associated to locomotion or other very common behaviors have been observed earlier in time [31, 32, 33]. Rapidly, the central nervous system has been recognized to process by different manners the two types of movements so that discrete movements appeared to be generated by more elaborate cortical areas [34, 35, 36] whereas rhythmic movements appeared to emanate from lower neuronal circuitries [8]. One of the oldest functional neural circuits is the spinal central pattern generator (CPG) – a circuit capable of generating rhythmic motor activity even when rhythmic input from the peripheral receptors is absent [37].

1.3.1. The brief history of CPG

In 1910, Sherringon and colleagues were the first in the field to discuss a alternating stepping behavior in cats and dogs generated by continuous stimuli in the spinal chord [38]. Later on, in 1911, Brown [39] introduced the concept of Central Pattern Generator (CPG). Brown also validated Sherrington's findings by conducting an experiment on cats having gone through thoracic spinal chord transection [39]. The experiment demonstrated rhythmic alternating contractions of flexor and extensor muscles in cats' ankles, suggesting the existence of a balanced center in the spinal chord that produces equal and opposite activation of antagonist muscles. This center is composed of two interconnected neural populations, each called "half-center", which requires a stimulus to act on a single half-center to engage the activation process.

At this stage of the research, the half-center oscillator pictured in Fig.1.1 is the original simple version of the CPG. Is it composed of two neurons, which act as mutual inhibitors. Considering that the two neurons -that have slightly different initial activation values- are simultaneously stimulated by a constant input, the neuron that has a lightly higher initial parameter will generate sequences of action potentials, and as the firing is happening, a inhibitory signal proportional to the firing will be sent by the first neuron to the second to impeach the second neuron from firing. The first neuron is then activated, and the second neuron is inhibited. Under the assumption that the neurons are subject to fatigue, the firing neuron will slowly decrease its activation, which will gradually reduce the inhibition acting on the second neuron, allowing the second to start firing. The same principle, under a constant stimulating input, will create alternating firing of each neurons

to produce a rhythmic movement.

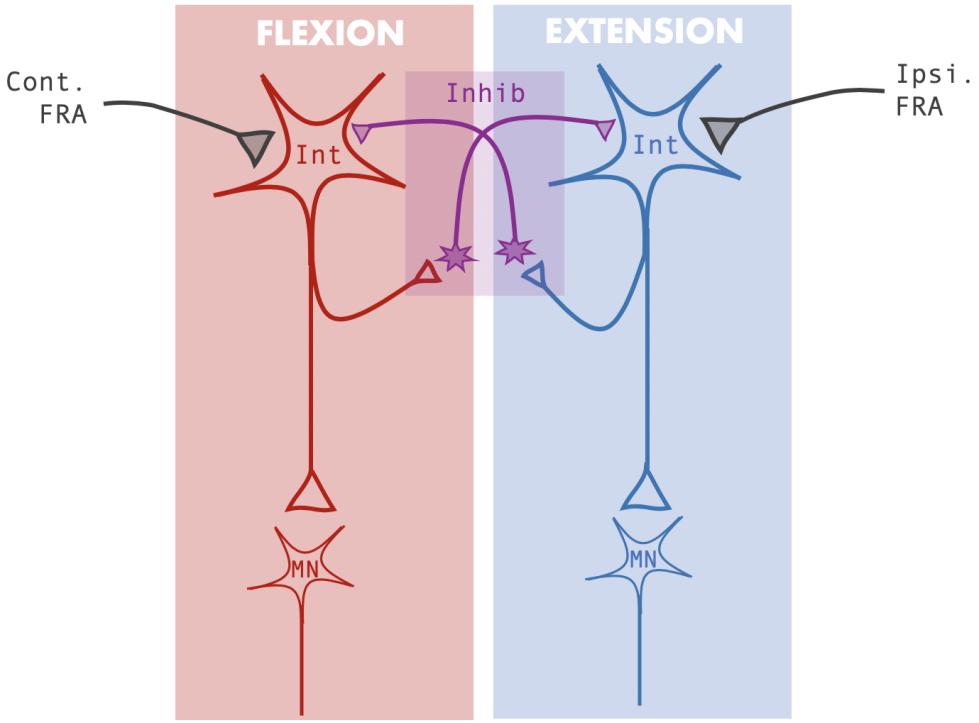

Figure 1.1. Basic Half-Center Oscillator representation with two self-inhibitory neurons under the assumptions that (1) the neurons are subject to fatigue and (2) the neurons have two slightly different initial conditions. FRA stands for Flexor Reflex Afferents, Int for Interneuron and MN for Motorneuron.

Other research studies have been conducted by Shik et al. [40] and Duysens et al. [41] on cats that undergone a spinal transection, called "Spinal Cats", highlighting similar lower-limb activation patterns. Between 1988 and 2005, many studies have largely supported the implication of the CPG at a spinal level for lower-limb rhythmic alternative activation in non-primate and primates, including humans [31, 32, 33, 41, 42, 43]. By conducting a study showing an induction of locomotory-like patterns when stimulating the spinal cord on human subjects presenting lumbar spinal cord injury, Dimitrijevic showed in 1998 evidence of presence of spinal CPG structures in humans [33].

While early research works on CPGs were mainly focused on lower-limb rhythmic

patterns, the concept has more recently been extended to rhythmic actions produced by the upper limbs by Dietz, [34, 44], Zehr et al. [36, 35], and White et al. [45]. Dietz suggested the existence of a cervical center coupled to the aforementioned thoraco-lumbar CPG center that allows humans the control of upper-limbs during locomotion. This association is reflected, among others explanations, by the coupled arms and legs-swings during human locomotor activities, and by an upper-limb Hoffmann's reflex or H-reflex (i.e. electronically induced muscle contraction) during lower-limbs rhythmic behaviors [46]. The work conducted by Zehr et al. [35] led to the observation that previously discussed H-reflex are modulated in a similar manner during upper and lower limb rhythmic movements, at the exception of the the amplitude modulation of the reflex during contralateral arm movement. Those findings suggest that rhythmic arm movements are, at least partially, controlled by the same CPG centers as lower-limbs during rhythmic activities. In another work conducted at the same time, Zehr et al. evidenced that, even tough both controlled by CPG, the coupling existing during upper limbs during rhythmic movements is weaker than the coupling existing between legs [36].

In 2004, a study conducted by Schaal et al. [8] reported differences in cortical areas activation during discrete and rhythmic wrist movements. Indeed, whilst performing discrete movements, participants showed activation of several higher cortical areas, in addition to the areas activated during the performance of rhythmic movements, which agrees with the two very distinct definitions of rhythmic and discrete movements. We now understand how rhythmic movements are generated through CPG centers, and to extend the discussion on generation of discrete movements, the *force field* concept needs to be introduced. Initially discussed by Bizzi through an experiment on surgically altered frogs,

the force field represent the field of all forces generated by muscles when stimulating the same area of the spinal chord [47]. The results of this study suggest that a small number of force fields, and a simple linear combinations of those force fields account for a large repertoire of motor behaviors. But while these frog movements are indeed "intelligent", supraspinal mechanisms are clearly involved in typical discrete reaching movements in humans [37]. In later work, Bizzi and colleagues expanded their findings, suggesting that the aforementioned linear combination strategy used in an organized manner could be used by the CNS to adapt a multitude of motor behaviors to the external environment [48]. Additional findings by Giszter et al. then suggested that modulating the intensity of the spinal cord stimulation would not affect the force field patterns [49], i.e. that the motor activity generation by the CNS is not as complicated as it initially seemed to be, and that those behaviors could account for discrete movements generation. A more extensive literature review on the topic has been written by Degallier and Ijspeert [50].

Now that behaviors that both describe the generation of rhythmic and discrete movements have been discussed, one can wonder how the two types of movements relate to each others. This is what Saltiel et al. attempted to assess in 1998 and 2005 [51, 52]. Both of those work highlighted the close activation areas for discrete and rhythmic movements, suggesting that rhythmic movements could be simply described as a combination of discrete movements, which could justify the use of CPG structures for the generation of discrete movements. Those findings were revolutionary in a manner that the difference in generation of discrete and rhythmic movements could reside in the modulation of features that describe each type of movement, i.e. discrete movements could be encoded by a target position and a onset timing whereas a rhythmic movement could be encoded by a

frequency and a phase.

Whilst unimanual rhythmic and discrete movements have been widely studied, a large component of the research in the field has been devoted to bimanual activities, more precisely to the effect of bimanual rhythmic/rhythmic patterns as well as rhythmic/discrete activities. As emphasized in the introduction, bimanual rhythmic/discrete activities are largely represented in daily activities, and studying the impact of one on another is important to understand coordination in bimanual motor tasks. If one name had to be cited to represent bimanual rhythmic/rhythmic or discrete/discrete research studies, it should be Kelso [53, 26], and if one review should be recommended on this topic, it would be Sternad's one [54]. Indeed, the interaction of bimanual similar movements has been widely discussed, but the interests here are carried toward the interaction of discrete and rhythmic movements. An experiment conducted by Goodman and Kelso explored the effects of a rhythmic movement in the synchronous initiation of a discrete movement [55], and the results suggested that the initiation of a discrete movement is more likely to happen during the velocity peak of a rhythmic movement.

Findings discussed in this section suggested that CPG are well identified, and their functioning has been elucidated, which led researchers to modeling CPGs. The next section will go through the development of models to simulate discrete and rhythmic movements.

1.3.2. CPG: Simulations and Modeling

Between 1985 and 1997, at the time when no direct evidence accounted for the existence of CPGs in humans, Matusoka, Nagashino et al., and Grossberg et al. [56] worked

on modeling the basic concept of CPGs, i.e. a circuit separated in two symmetrical and mutually inhibitory structures (pair of antagonist muscles)-termed a half-center oscillator, as illustrated in Figure 1.1. Indeed, Matusoka gave his name to a still widely represented Matusoka oscillator, that generates rhythmic activity when a constant input is provided into the circuit. The key to emergence of rhythm from the elements that are not rhythmic themselves is mutual inhibition present between two neural populations subject to fatigue [57, 58]. Following this first introduction to CPG half-center oscillator, Nagashino and Kelso [59, 60] aimed their research to understanding biological phase modulation behaviors during rhythmic activities. In 1985, at the time where the model by Haken, Kelso and Bunz was introduced [2], the distinction of in-phase and anti-phase stable and unstable modes under specific conditions by introducing self positive feedback loop to the excitatory neuron in addition to the negative inter-neurons feedback loop was made. At this point in time, many CPG models have been developed, simulating swimming activities [61], snail feeding networks [62], or even salamander swimming and walking activities [63]. Many models have been developed, but a similitude can be observed among them, i.e. the usage of two symmetrical mutually-inhibitory CPG structures. Starting in 2000, a new approach of CPG models arose, those incorporating a optimization principles to assess the neural processes of planning, control and sensory feedback [64, 65]. Those models modulating the behavioral information sent by the CNS with sensory information given from the effector. One solution offered by Flash and Hogan consisted in minimizing the effector jerk in reaching movements [66]. The development of such new approaches allowed the models to better represent biologically observed motor activities. More recently, between 2000 and 2008, Sternad, De Rugy, Wei, Ronsee and their colleagues investigated the in-

corporation of rhythmic/discrete interactions in models so that unexpected perturbations or other visual or auditory stimulations could be represented [67, 68, 69, 70]. While traditionally CPG circuits have been hypothesized to mediate rhythmic activities of the lower limb, recent evidence suggests that similar circuity may be used by the CNS in regulation of rhythmic upper limb movements [35].

Chapter 2. Methods

2.1. Matusoka Oscillator

For this study, the model developed by Ronsee et al. based on the half-center Matusoka oscillator [1] will be used. The model consisting in two antagonist groups of neurons allows to control a simple one degree of freedom rhythmic movement when stimulated by a constant input. The magnitude of input into the network determines the amplitude of the rhythmic movement. The model has been simulated using Simulink R2020a (MathWorks, Natick, MA) and the results have been driven using Matlab R2020a (MathWorks, Natick, MA). The generated Simulink diagrams can be found in the Appendix B, Figures B.1, B.2, B.3, B.4.

2.1.1. Unimanual Rhythmic Movement

The dynamic of the Matsuoka oscillator is based on a set of two differential equations (Eq. 2.1) that model the rate of discharge (Ψ_i and Ψ_j) of the two neurons, respectively.

$$\begin{cases} t_1\dot{\Psi}_i = -\Psi_i - \beta\phi_i - \eta[\Psi_j]^+ + u_i \\ t_1\dot{\Psi}_j = -\Psi_j - \beta\phi_j - \eta[\Psi_i]^+ + u_j \end{cases} \tag{2.1}$$

$\dot{\Psi}_i$ and $\dot{\Psi}_j$ are the firing rates of each neuron, t_1 is the time constant for the discharge rate -rate at which the electrical signals are sent from the neuron to the effector-, β is the constant of self-inhibition, and η is the constant of mutual inhibition. $[\Psi_j]^+$ and $[\Psi_i]^+$ denote that only the positive values of the rate of discharge are being considered for mutual inhibition terms. The self-inhibition is controlled by ϕ_i and ϕ_j, two other state-variables respecting the following equations (Eq. 2.2) from which the fatigue (or adaptation) is described. Fatigue is mostly known as the muscular fatigue after an intense or pro-

longed effort, but the term fatigue here refers to the neural fatigue that leads to a decrease in the rate of firing of a neuron. The fatigue in neuronal discharge cause by the Central Nervous System internal processes referred to as synaptic fatigue generated by a decrease of the number of synaptic vesicles in charge of neurotransmitters release; neurotransmitters without which a signal cannot be transmitted to a neuron nor a muscle.

$$\begin{cases} t_2\dot{\phi}_i = -\phi_i + [\Psi_i]^+ \\ t_2\dot{\phi}_j = -\phi_j + [\Psi_j]^+ \end{cases} \tag{2.2}$$

with t_2 being the fatigue (or adaptation) phenomenon's time constant [61]. The adaptation of the neuron's discharge rate is closely linked to external input $u(t)$ given to the system. The rate of discharge will rapidly increase to a maximum value governed by t_1 and slowly decrease to a value over a timescale given by t_2.

Considering that each half-center of the Matusoka oscillator is responsible for the muscle activation of antagonistic muscles of a single joint, the rates of discharge Ψ_i and Ψ_j are assumed to be proportional to the level of muscle activation of the antagonistic muscles. The muscle activation produce torques about the axis of rotation of the joint. The total torque about the joint follows the equation given be Eq. 2.3 where h_Ψ is the torque gain.

$$\Psi_T = h_\Psi([\Psi_i]^+ - [\Psi_j]^+) \tag{2.3}$$

The kinematic parameters of the effector are estimated through conversion of the torque into velocity according to the second-order mechanical system equation (Eq. 2.4), where I is the moment of inertia of the system and γ is the damping. θ and its first and second time derivatives ($\dot{\theta}$ and $\ddot{\theta}$ respectively) denote the effector angular position, velocity

and acceleration. The model of the effector does not include the stiffness term.

$$I\ddot{\theta} + \gamma\dot{\theta} - \Psi_T = 0 \tag{2.4}$$

In section 1.3.2 I have described that Matusoka and other CPG models have evolved by integrating proprioceptive feedback in the simulations. This sensory feedback biologically represents afferent information that emerges from muscles spindles - special kinds of sensory muscle fibers involved in monosynaptic stretch reflex- and travels through ascending pathways to the spinal chord [33, 71]. With the integration of the sensory feedback to the system, the sets of equations (Eq. 2.1) are transformed by incorporating a sensory coupling term where the parameter σ corresponds to the strength of the sensory coupling and $\theta^\star$ is the reference angular position of the effector around which the effector oscillates:

$$\begin{cases} t_1\dot{\Psi}_i = -\Psi_i - \beta\phi_i - \eta[\Psi_j]^+ - \sigma[\theta - \theta^\star]^+ + u_i \\ \\ t_1\dot{\Psi}_j = -\Psi_j - \beta\phi_j - \eta[\Psi_i]^+ - \sigma[\theta^\star - \theta]^+ + u_j \end{cases} \tag{2.5}$$

The Matusoka oscillator, as described by the sets of equations presented in this section, produces a single-limb oscillatory rhythmic movement. In the following section the adaptation of this model to produce a discrete movement will be described.

2.1.2. Unimanual Discrete Movement

It has been discussed in section 1.3.2 that CPG models can be used to simulate discrete movements as well as rhythmic movements. The key here is that instead of constant, non-specific input, the CPG circuit needs to receive a more complicated input pulse. If the pulse is properly timed and scaled, the CPG circuit produces the motion of the effector that starts from a posture and comes to a stop at a new posture – i.e., performs a discrete movement [5]. For the case of the Matusoka Oscillator described here, giving to the

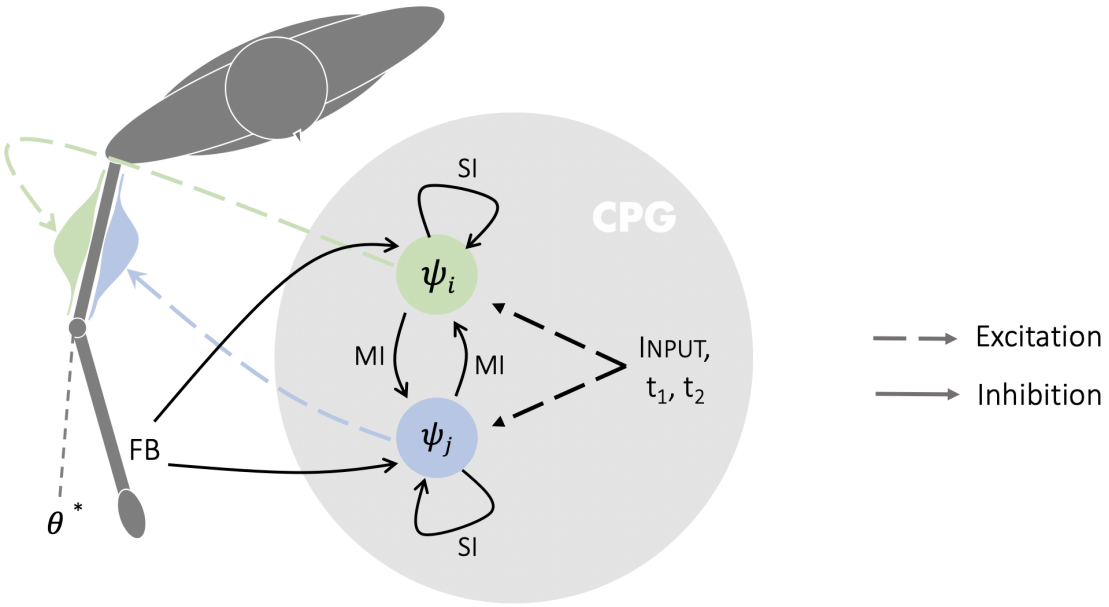

Figure 2.1. Representation of Matusoka oscillator for unimanual activities. The CPG model allows to control two antagonistic muscles, here the biceps and triceps that control a one degree-of-freedom rotation at the elbow joint when alternatively activated. Solid arrows represent inhibitory signals and dashed arrows represent excitatory signals. $\Psi_{i,j}$ denote the rate of discharge of neurons i, j, SI: self-inhibition, MI: mutual inhibition, FB: sensory feedback.

model an input following the equation Eq. 2.6 originally proposed by de Rugy and Sternad [68] that generates a ballistic discrete movement, where $\theta^\star$ is the amplitude of the discrete movement, τ is the duration of the movement, and t_0 is the movement onset timing. The parameters of this equation has been obtained from fitting many inputs computed by dynamical inversion [1].

$$u_p(t) = \left[0.07\frac{|\theta^\star|}{\tau}\left(e^{\frac{1.4(t-t_0)}{\tau}} - 1\right)e^{\frac{-4.1(t-t_0)}{\tau}}\right]^+ \tag{2.6}$$

2.1.3. Bimanual Movements Generated by the Model

Up to this point, only unimanual movement generation of rhythmic and discrete movements have been described. In the current section, I will describe the model that adds a second effector and incorporates inter-limb "coupling" to model movement produc-

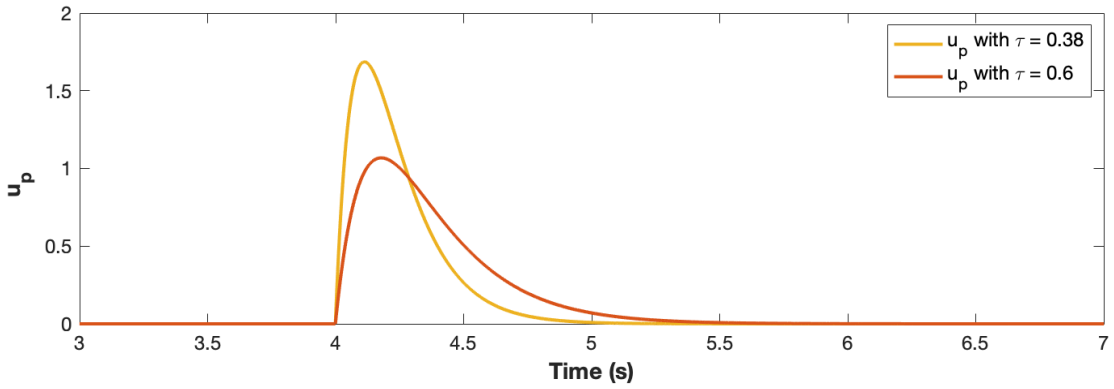

Figure 2.2. Graphical representation of the discrete movement input $u_p(t)$ function, with two different τ values.

tion during bilateral activities.

The two mechanical second-order systems represented by this model are driven by two separate CPG centers that have a structure identical to the unimanual CPG model. The dynamical coupling terms representing the inter-limb interaction are added to the model at the θ_r and θ_l level to account for the interaction between the two limbs in the afferent pathway. θ_r is coupled with $\psi_{r,i}$ and $\psi_{r,j}$ to account for the homologous coupling, and $\psi_{l,i}$ and $\psi_{l,j}$ for non homologous coupling. The coupling is identical for θ_l, using symmetrical terms. r and l underscores respectively denote the characteristics of the right and left effectors. Equations 2.7 and 2.9 respectively represent the firing rate of the coupled right and left effectors; and Equations 2.8 and 2.10 respectively dictate the self-inhibition state variables of each effectors, with t_1 and t_2 parameters being identical for each limb. Those parameters, as described in [1], are defined with the same values for unimanual activities in the computational model.

$$\begin{cases} t_1\dot{\Psi}_{r,i} = -\Psi_{r,i} - \beta\phi_{r,i} - \eta[\Psi_{r,j}]^+ - \sigma[\theta_r - \theta_r^\star]^+ - \mu[\theta_l - \theta_l^\star]^+ - \nu[\theta_l^\star - \theta_l]^+ + u_{r,i} \\ t_1\dot{\Psi}_{r,j} = -\Psi_{r,j} - \beta\phi_{r,j} - \eta[\Psi_{r,i}]^+ - \sigma[\theta_r^\star - \theta_r]^+ - \mu[\theta_l^\star - \theta_l]^+ - \nu[\theta_l - \theta_l^\star]^+ + u_{r,j} \end{cases} \tag{2.7}$$

$$\begin{cases} t_2\dot{\phi}_{r,i} = -\phi_{r,i} + [\Psi_{r,i}]^+ \\ t_2\dot{\phi}_{r,j} = -\phi_{r,j} + [\Psi_{r,j}]^+ \end{cases} \tag{2.8}$$

$$\begin{cases} t_1\dot{\Psi}_{l,i} = -\Psi_{l,i} - \beta\phi_{l,i} - \eta[\Psi_{l,j}]^+ - \sigma[\theta_l - \theta_l^\star]^+ - \mu[\theta_r - \theta_r^\star]^+ - \nu[\theta_r^\star - \theta_r]^+ + u_{l,i} \\ t_1\dot{\Psi}_{l,j} = -\Psi_{l,j} - \beta\phi_{l,j} - \eta[\Psi_{l,i}]^+ - \sigma[\theta_l^\star - \theta_l]^+ - \mu[\theta_r^\star - \theta_r]^+ - \nu[\theta_r - \theta_r^\star]^+ + u_{l,j} \end{cases} \tag{2.9}$$

$$\begin{cases} t_2\dot{\phi}_{l,i} = -\phi_{l,i} + [\Psi_{l,i}]^+ \\ t_2\dot{\phi}_{l,j} = -\phi_{l,j} + [\Psi_{l,j}]^+ \end{cases} \tag{2.10}$$

The sensory coupling between the two effectors is introduced through μ and ν, inhibitory parameters that respectively describe homologous and non-homologous muscle couplings, both being function of the contralateral limb.

2.1.4. Bimanual Discrete/Rhythmic Coupling

In Ronsee's CPG model, the rhythmic/discrete bimanual coupling is developed based on the approach described in Section 2.1.3 [1]. The inputs given to the system for both limbs will determine the behavior adapted by the system. Equation 2.6 describes the input given for the limb performing the discrete movement whereas the input is a constant for the limb performing the rhythmic movement. The two assumptions governing this bimanual approach are (1) the discrete movement can be initiated at any timing in the phase of the rhythmic movement, and (2) the rhythmic movement will be perturbed by the initiation of the discrete movement, with a perturbation effect that varies depending on the rhythmic movement's phase at which the perturbation occurs [1].

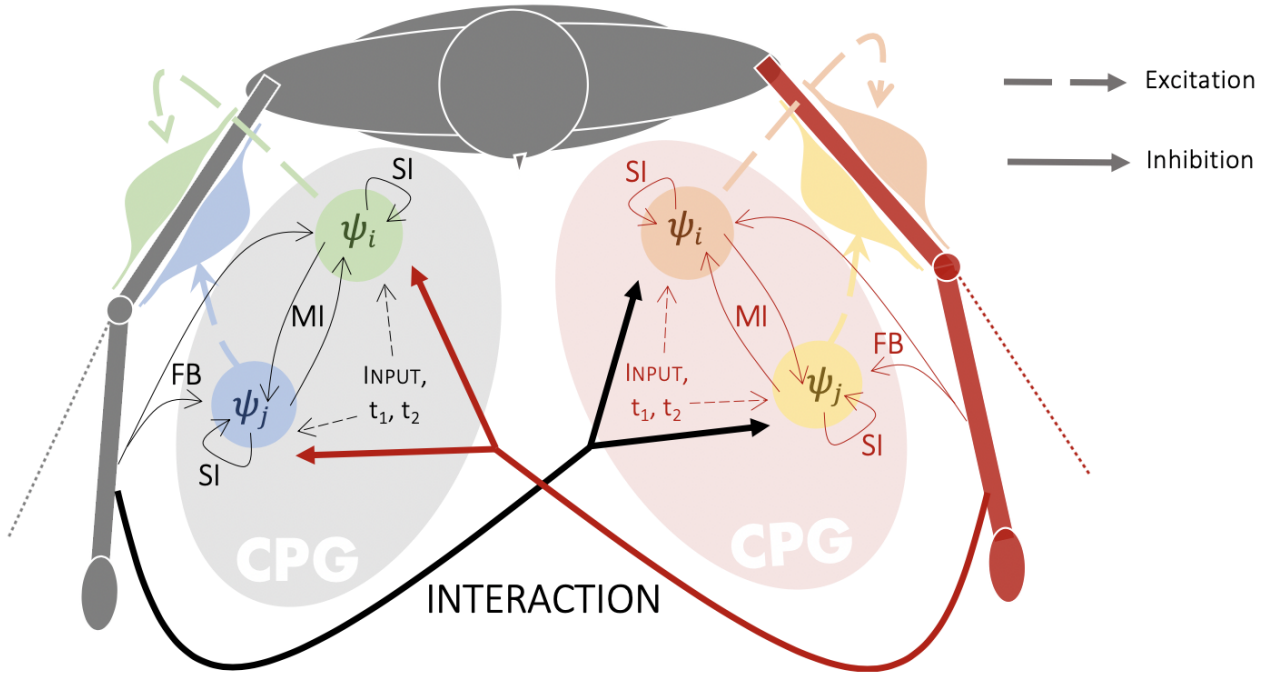

Figure 2.3. Representation of Matusoka CPG oscillator model for bimanual activities. The excitatory signals are represented by dashed arrows, and the inhibitory signals are represented by solid arrows. The details of each individual CPG center can be found in Fig. 2.1.

2.1.5. Choice of the model's parameters

Most of the parameters used for simulating the experiment were used as in Ronsse's document [1]. The duration of the discrete movement, is manipulated by changing the movement duration τ in eq. 2.6. I then determined the value of τ to obtain a peak velocity of the discrete movement roughly 20% above or below the peak velocity of the rhythmic movement for the fast or slow conditions, respectively. Figure 2.4 displays the peak velocities of the discrete movement under the Slow and Fast conditions. With a duration of the fast discrete (FD) movement of $\tau = 0.38$ s, the peak velocity of the discrete movement is $\omega_{FD_{max}} = 2.85$ rad/s (i.e. 163.3 deg/s), or 18.6 % smaller than the peak velocity of the rhythmic movement. With a duration of $\tau = 0.6$ s, the slow discrete (SD) movement has a peak velocity of $\omega_{SD_{max}} = 4.35$ rad/s (i.e. 249 deg/s), or 24.2% higher

than the peak velocity of the rhythmic movement. All the parameters used for the simulation are presented in Table 2.2 and Table 2.1. The period T and the input u_T of the rhythmic movement have been calculated using Equations 2.12 2.13, 2.11 with $A_\theta = 35$ deg.

$$\begin{cases} t_1 = 2.13 + 0.6804T - \sqrt{4.512 + 2.685T} \\ t_2 = 2.5t_1 \end{cases} \tag{2.11}$$

$$u_T = \frac{A_\theta}{-323t_1^2 + 361t_1 - 6.306} \tag{2.12}$$

$$T = 1.47t_1 + 2.92\sqrt{t_1} - 0.2304 \tag{2.13}$$

Table 2.1. Simulation parameters specific to each limb, determined from the equations given in section 2.1.5.

Right Limb Rhythmic movement	**Left Limb Discrete movement**	
$u_T = 1.6$	**Fast Condition**	**Slow Condition**
$\theta^\star = 35$ deg $\omega_{R_{max}} = 3.5\ rad.s^{-1}$	$\tau = 0.38$ s $\omega_{FD_{max}} = 4.35\ rad.s^{-1}$	$\tau = 0.6$ s $\omega_{SD_{max}} = 2.85\ rad.s^{-1}$
$T = 0.5$s	$\theta^\star = 60$ deg	

I wanted to examine the effect of phase of discrete movement initiation on the rhythm. To accomplish that, another parameter that needs to be fed to the model is the timing at which the discrete movement is started. Under both fast and slow condition, the rhythmic/discrete interference was evaluated for a discrete movement that is initiated at different phases of the rhythmic movement. Figure 2.5 and Table 2.3 depicts the timings at which the discrete movement will be initiated, which have been decided to be at remarkable points of the rhythmic arm's velocity profile.

Table 2.2. General simulation parameters as in [1]

General parameters of the model
$t_1 = 0.05$ s
$t_2 = 0.125$ s
$\mu = 0.3$
$\nu = 0.15$
$\eta = 2.5$
$\gamma = 0.5\ Nm.s/rad$
$\beta = 2.5$
$I = 0.08\ Nm.s^2/rad$
$\sigma = 1.2$

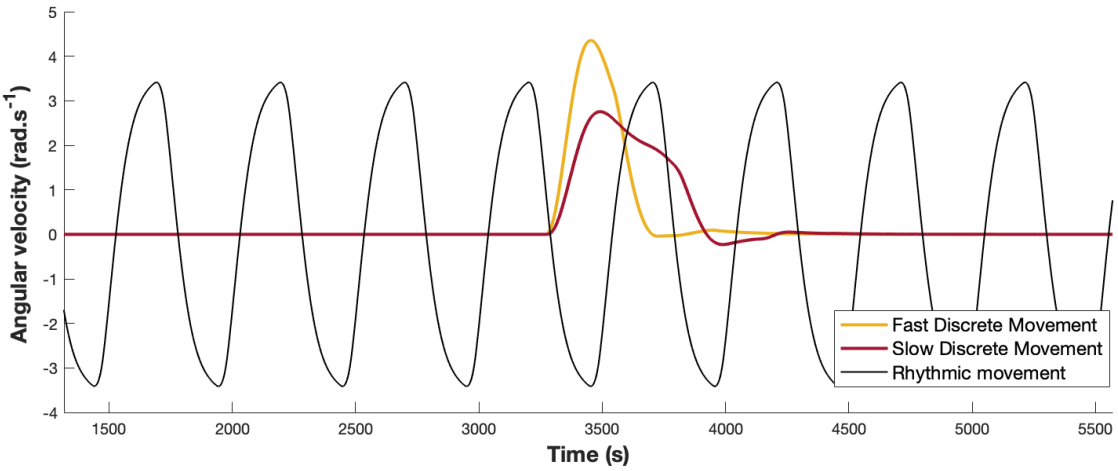

Figure 2.4. Peak velocities in $rad.s^{-1}$ for the rhythmic movement (in black), for the Slow discrete condition (in red), and for the Fast discrete condition (in yellow)

2.2. Dependent measures

There are two hypotheses to be tested in this study: (1) the velocity assimilation between both limbs during rhythmic-discrete interference would affect the extent of interference and (2) the co-contraction should increase during the perturbation (initiation of the discrete movement).

To test the first hypothesis, three dependent variables were evaluated: (1) the period shift, (2) the amplitude shift and (3) the phase reset of the rhythmic movement. Figure 2.6 depicts the definition of the three variables. The period of the rhythmic movement,

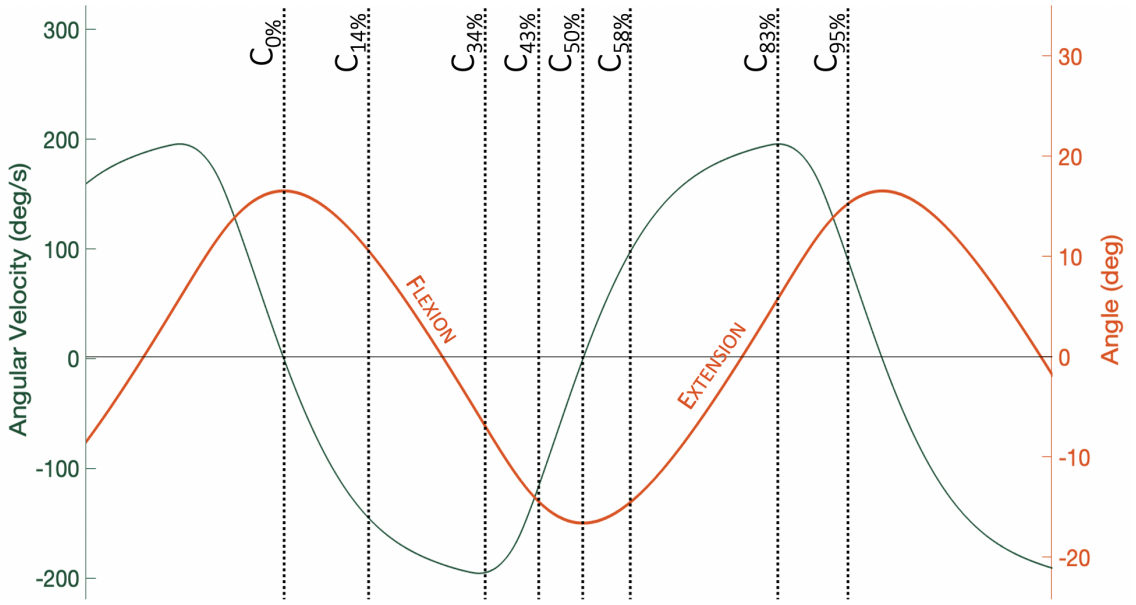

Figure 2.5. Conditions on the phase on the rhythmic movement at which the discrete movement occurs. In pink, the position (angle in rad) of the rhythmic limb, in blue, the velocity profile of the rhythmic limb, and in dashed black lines, the conditions on the phase. Table 2.3 details the velocity and position of the rhythmic limb for each condition.

in blue in Figure 2.6 will be calculated between each extension peaks (i.e. maximum angles) of the rhythmic movement, and the amplitude, in purple in Figure 2.6 will be calculated between each extension and preceding flexion peaks (i.e. Maximum and minimum angle) of the rhythmic movement. The phase reset of the rhythmic movement will be calculated by subtracting and dividing by 2π the extension peak value of the rhythmic movement to the extension peak value of the expected rhythmic movement if the perturbation had not occurred. The unperturbed rhythmic movement without occurrence of the discrete movement is drawn in dashed red line in Figure 2.6. A negative phase reset denotes a rhythmic movement that anticipates an oscillation compared to the rhythmic movement alone without the influence of the perturbation; and a positive phase reset denotes a rhythmic movement being delayed compared to the not-perturbed reference rhythmic

Table 2.3. Correspondence of each condition on the phase of the rhythmic movement at which the discrete movement occurs to the timing, the velocity profile and the type of movement performed by the rhythmic limb. Figure 2.5 is a visual representation of these information.

Condition	**Discrete Movement Timing (s)**	**Velocity Profile**	**Movement**
$C_{0\%}$	4.295	Null	Extension max.
$C_{14\%}$	4.366	Negative - Decreasing	Flexion
$C_{34\%}$	4.464	Minimum	Flexion
$C_{43\%}$	4.509	Negative - Increasing	Flexion
$C_{50\%}$	4.546	Null	Flexion max.
$C_{58\%}$	4.586	Positive - Increasing	Extension
$C_{83\%}$	4.710	Maximum	Extension
$C_{95\%}$	4.779	Positive - Decreasing	Extension

movement.

To test the second hypothesis, the co-contraction level will be estimated by evaluating the overlap of the right limb's flexor and extensor's neuron activation in the Matsuoka oscillator. The output from the oscillator, ψ_i, represents the amount of activation to the agonist and antagonist muscle groups. The area in common between firing rate of each neuron, denoted by ψ_i and ψ_j and plotted in blue and red in Figure 2.7 is called co-contraction area -in yellow in Figure 2.7- and will be calculated to evaluate the co-contraction level of the limb performing the rhythmic movement, shown in green in Figure 2.7. As seen on the figure in light pink, the muscle co-contraction happens during each velocity peak of the both flexion and extension movement. This co-contraction allows to "slow-down" the movement before the generation of the following flexion/extension of the limb.

The simulated model is deterministic, so no statistical analysis was required to evaluate changes in the model outputs.

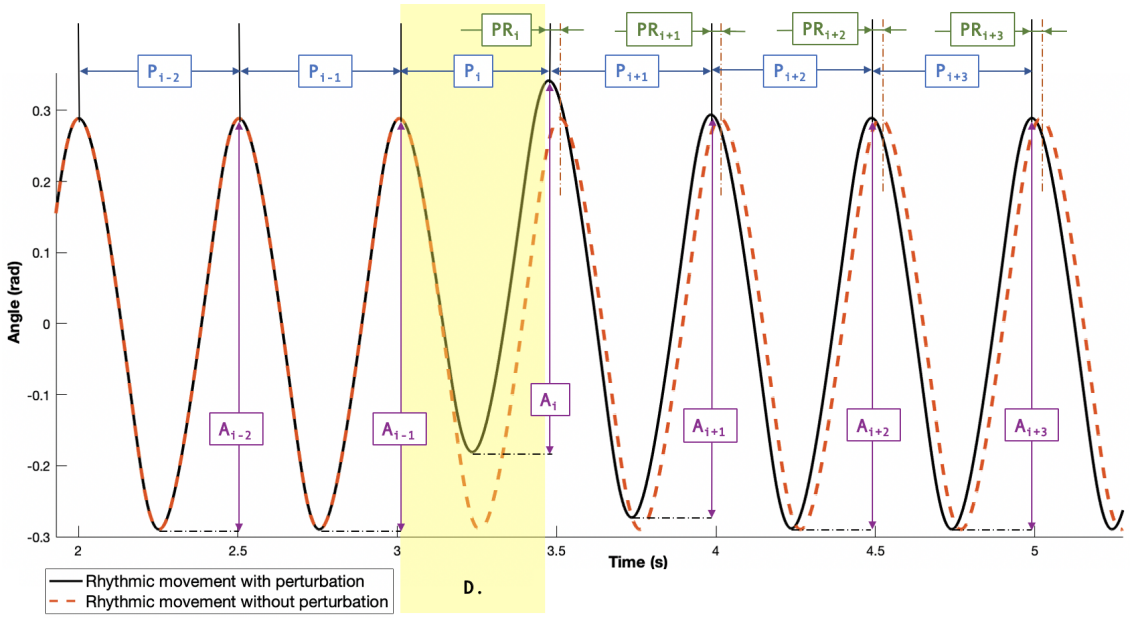

Figure 2.6. Visual representation of a rhythmic movement under the influence of the discrete movement (in solid black line), and without perturbation (in dashed red line). The three dependent variables are as follow: (1) amplitude at each oscillation in purple, (2) in blue the definition of the period, and (3) in green, the definition of the phase reset. The i^{st} oscillation being the oscillation during which the discrete movement occurs ($D.$), indicated by the yellow area.

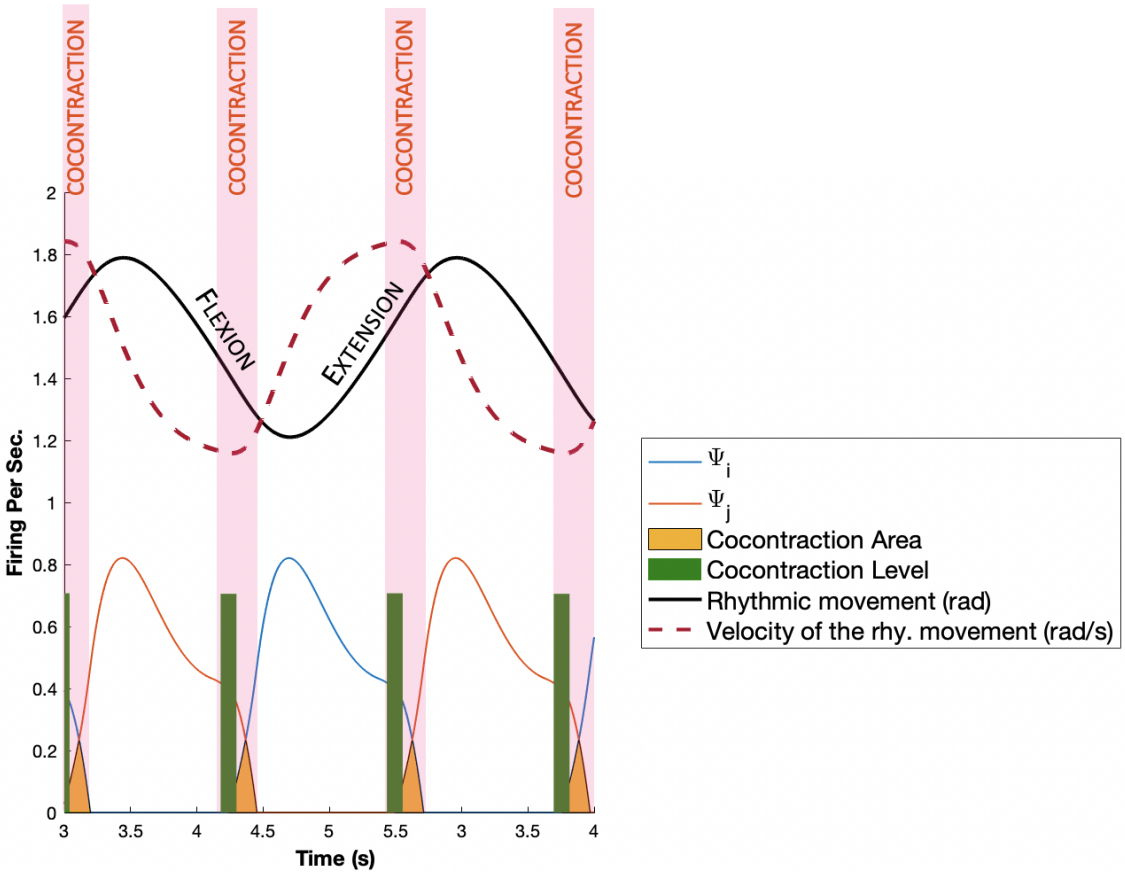

Figure 2.7. Visual representation of the firing of each antagonist neurons ψ_i and Ψ_j, respectively in blue and red, during one cycle and a half of the rhythmic movement. In yellow, the co-contraction area corresponds to the visual area on which the two neuron's firing rate are overlapping, and in green, the co-contraction level corresponds to the co-contraction area value. The pink areas shows the areas of the movement during which the co-contraction occurs.

Chapter 3. Results

The behavior of four dependent variables characterizing bimanual interference between rhythmic and discrete upper limb movements was evaluated under two different velocities of the discrete movement, and as a function of eight different phases of initiation of the discrete movement within the rhythmic cycle. The effects of discrete movement velocity on the kinematics of the rhythmic movement (period shift, amplitude shift, phase shift) are presented in the first section of the results chapter. The second section of the current chapter presents the results on the changes in the the estimated co-contraction level of the rhythmic limb.

3.1. Kinematic changes of the rhythmic movement

3.1.1. Period Shift

Figure A.5 and Table 3.1 depicts changes in the period of rhythmic movement immediately following the initiation of the discrete movement in the Fast condition (+20 percent faster than the rhythmic peak velocity). The baseline period was $0.50s$, and the results showed that the initiation of the discrete movement at $C_{0\%}$ to $C_{83\%}$ immediately influenced the rhythmic oscillation during which the perturbation occurs, whereas under $C_{95\%}$, the influence was delayed to next oscillation cycle $i + 1$ following the perturbation. When the discrete movement was initiated at $C_{0\%}$, $C_{14\%}$ and $C_{95\%}$, the rhythmic movement became faster (i.e. period of the oscillation decreased to $0.47s$ for $C_{0\%}$ and $C_{14\%}$ and $0.48s$ for $C_{95\%}$) before speeding up and getting back to the baseline period of $0.50s$. For the conditions $C_{34\%}$ to $C_{83\%}$, the period of the oscillation i increased to $0.52s$ for $C_{34\%}$ to $C_{58\%}$, and to $0.51s$ for $C_{83\%}$. Looking at the number of oscillations affected by the pertur-

bation, $C_{34\%}$ and $C_{43\%}$ are the least affected by the discrete movement, since the rhythmic movement returned to its baseline period after only one full movement cycle. $C_{83\%}$ is the condition under which the rhythmic movement was the most affected by the perturbation since the rhythmic movement returned to the baseline after three oscillations. An interesting observation is that the magnitude of the period shift is not related to the number of oscillations during which the rhythmic movement is perturbed, which can be observed from the behavioral differences between $C_{34\%}$ and $C_{83\%}$. The magnitude of the shift was higher for $C_{34\%}$, but the rhythmic movement returned back to its baseline value faster than for $C_{83\%}$ that overcomes a small shift in magnitude.

Table 3.1. Period in the Fast condition. Values in red show an increase of the period -i.e. rhythmic movement slowing down- whereas values in blue show a decrease of the period -i.e. speeding up-.

	$C_{0\%}$	$C_{14\%}$	$C_{34\%}$	$C_{43\%}$	$C_{50\%}$	$C_{58\%}$	$C_{83\%}$	$C_{95\%}$
$i-1$	0.50	0.50	0.50	0.50	0.50	0.50	0.50	0.50
i	0.47	0.47	0.52	0.52	0.52	0.52	0.51	0.50
$i+1$	0.51	0.51	0.50	0.50	0.51	0.51	0.50	0.48
$i+2$	0.50	0.50	0.50	0.50	0.50	0.50	0.51	0.51
$i+3$	0.50	0.50	0.50	0.50	0.50	0.50	0.50	0.50
$i+4$	0.50	0.50	0.50	0.50	0.50	0.50	0.50	0.50

A similar pattern of results occurred for the slow discrete movement condition as shown in Figure A.6 and Table 3.2. Indeed, the rhythmic movement showed a transient adaptation of the period before returning to baseline for $C_{0\%}$, $C_{14\%}$, $C_{83\%}$ and $C_{95\%}$, under which the rhythmic movement showed a speeding-up, then a slowing-down before returning to the baseline period. One major noticeable difference between the fast and slow conditions is the effect $C_{34\%}$ and $C_{43\%}$ have on the number of oscillations the rhythmic movement needs to return to baseline period to one only.

Table 3.2. Period under slow condition (s). Values in red show an increase of the period -i.e. rhythmic movement slowing down- whereas values in blue show a decrease of the period -i.e. speeding up-.

	$C_{0\%}$	$C_{14\%}$	$C_{34\%}$	$C_{43\%}$	$C_{50\%}$	$C_{58\%}$	$C_{83\%}$	$C_{95\%}$
$i-1$	0.50	0.50	0.50	0.50	0.50	0.50	0.50	0.50
i	0.47	0.47	0.52	0.53	0.52	0.52	0.51	0.50
$i+1$	0.51	0.51	0.50	0.50	0.50	0.50	0.49	0.48
$i+2$	0.50	0.50	0.50	0.50	0.50	0.50	0.51	0.51
$i+3$	0.50	0.50	0.50	0.50	0.50	0.50	0.50	0.50
$i+4$	0.50	0.50	0.50	0.50	0.50	0.50	0.50	0.50

Overall, change in the period of the rhythmic movement depended on when within the rhythmic cycle ($C_{0\%}$ to $C_{95\%}$) the discrete movement was initiated, but not on the velocity of the discrete movement. Initiation of discrete movement at $C_{83\%}$ had the strongest influence, both for Fast and Slow conditions, whereas $C_{34\%}$ and $C_{43\%}$ were the least affecting the rhythmic movement. $C_{50\%}$ and $C_{58\%}$ have variable effects on the rhythmic movement depending on the velocity condition on the discrete movement.

3.1.2. Amplitude Shift

The amplitude shift results under the Fast condition of the discrete movement are presented in Figure A.5 and in Table 3.3. The baseline amplitude was 0.58 rad. Those results show that for $C_{0\%}$, the amplitude decreases to $0.49rad$, and for $C_{14\%}$ and $C_{95\%}$, the amplitude decreased to a minimum of 0.51 rad. For all the conditions but $C_{95\%}$, the shift occurred in the i^{st} oscillation, and the amplitude would return to baseline value after two oscillations for $C_{0\%}$, $C_{14\%}$, $C_{95\%}$, three oscillations for $C_{83\%}$, and one oscillation for $C_{34\%}$ to $C_{58\%}$. For $C_{34\%}$ to $C_{83\%}$, the amplitude of the i^{st} oscillation was slightly increased by $0.01rad$ to 0.03 rad before returning to baseline value of 0.58 rad. $C_{0\%}$ is the condition under which the magnitude of the rhythmic movement is the most reduced with a peak shift

of 0.09 rad.

Table 3.3. Amplitude under fast condition (rad). Values in red show an increase of the amplitude whereas values in blue show a decrease of the amplitude.

	$C_{0\%}$	$C_{14\%}$	$C_{34\%}$	$C_{43\%}$	$C_{50\%}$	$C_{58\%}$	$C_{83\%}$	$C_{95\%}$
$i-1$	0.58	0.58	0.58	0.58	0.58	0.58	0.58	0.58
i	0.49	0.51	0.59	0.60	0.59	0.59	0.61	0.58
$i+1$	0.56	0.56	0.58	0.58	0.58	0.58	0.54	0.51
$i+2$	0.58	0.58	0.58	0.58	0.58	0.58	0.57	0.56
$i+3$	0.58	0.58	0.58	0.58	0.58	0.58	0.58	0.58
$i+4$	0.58	0.58	0.58	0.58	0.58	0.58	0.58	0.58

As for the Slow condition, the results on the amplitude shift are displayed in Figure A.6 and in Table 3.4. Under $C_{0\%}$, $C_{14\%}$, $C_{34\%}$ and $C_{95\%}$, the results suggest that the rhythmic movement is affected for two oscillations following the discrete movement initiation, with a maximum decrease of the amplitude of $0.09rad$ for $C_{0\%}$, $0.07rad$ for $C_{14\%}$ and $0.08rad$ for $C_{95\%}$. $C_{34\%}$ to $C_{83\%}$ show the same pattern of an amplitude slightly increasing during the i^{st} oscillation between 0.01 and $0.03rad$, and decreasing during oscillation $i+1$, to slowly getting back to the baseline amplitude at oscillations $i+2$ for $C_{43\%}$ and $i+3$ for the other conditions.

Table 3.4. Amplitude under slow condition (rad). Values in red show an increase of the amplitude whereas values in blue show a decrease of the amplitude.

	$C_{0\%}$	$C_{14\%}$	$C_{34\%}$	$C_{43\%}$	$C_{50\%}$	$C_{58\%}$	$C_{83\%}$	$C_{95\%}$
$i-1$	0.58	0.58	0.58	0.58	0.58	0.58	0.58	0.58
i	0.49	0.51	0.60	0.60	0.60	0.59	0.61	0.58
$i+1$	0.56	0.56	0.57	0.56	0.55	0.55	0.51	0.50
$i+2$	0.58	0.58	0.58	0.57	0.57	0.57	0.56	0.56
$i+3$	0.58	0.58	0.58	0.58	0.58	0.58	0.58	0.58
$i+4$	0.58	0.58	0.58	0.58	0.58	0.58	0.58	0.58

The results suggest that $C_{0\%}$, $C_{14\%}$, $C_{83\%}$ and $C_{95\%}$ are affecting the rhythmic movement roughly in the same way under the Slow and Fast conditions. Nevertheless,

under $C_{34\%}$ to $C_{58\%}$, the results showed a better adaptation of the rhythmic movement under the Fast condition rather than the Slow condition.

3.1.3. Phase Reset

The phase reset for the Fast Condition is presented in Figure A.5 and in Table3.5. Overall, all the conditions on the phase of the rhythmic movement during which the discrete movement occurs underwent a phase reset for the remaining of the trials. $C_{14\%}$ is the condition that affected the rhythmic movement the most, with a final phase reset of $-0.006s/rad$ and $C_{95\%}$ was the condition that affected the least the rhythmic movement with a final phase reset of $-0.002s/rad$. Nevertheless, there was a transient effect observed for all the conditions but $C_{50\%}$. $C_{0\%}$, $C_{14\%}$ and $C_{95\%}$ showed a negative phase reset of $-0.007s/rad$ for $C_{0\%}$ and $C_{14\%}$, and $-0.004s/rad$ for $C_{95\%}$. $C_{34\%}$, $C_{43\%}$, $C_{58\%}$ and $C_{83\%}$ showed a positive phase reset of 0.002 for $C_{83\%}$, $0.003s/rad$ for $C_{34\%}$ and $C_{58\%}$, and $0.004s/rad$ for $C_{43\%}$. $C_{0\%}$, $C_{83\%}$ and $C_{95\%}$ showed a transient perturbation of the rhythmic movement during two oscillations before reaching their final phase reset value, and the other conditions but $C_{50\%}$ showed a transient perturbation effect during only one oscillation. All the conditions perturbed the rhythmic movement during the oscillation i where the discrete movement occurred, but $C_{95\%}$ perturbed the rhythmic movement at the oscillation $i+1$.

Phase reset in the slow discrete movement condition are shown in Figure A.6 and in Table 3.6. All the conditions induced a reset of the phase of the rhythmic movement until the end of the trial. Condition $C_{0\%}$ had the greatest impact on the rhythmic movement, inducing a final reset of $-0.005s/rad$, and $C_{83\%}$ has the least impact on the final

Table 3.5. Phase Reset in the Fast condition. Values in red show a positive shift of the phase with respect to the phase of a not-perturbed rhythmic movement -i.e. the rhythmic movement falls after the predicted value-. Values in blue show a negative shift of the phase of the rhythmic movement after the perturbation occurs -i.e. the rhythmic movement falls before the predicted value-. The values in yellow show the final constant reset of the phase after the recovery of the rhythmic limb from the perturbation.

	$C_{0\%}$	$C_{14\%}$	$C_{34\%}$	$C_{43\%}$	$C_{50\%}$	$C_{58\%}$	$C_{83\%}$	$C_{95\%}$
$i-1$	0.000	0.000	0.000	0.000	0.000	0.000	0.000	0.000
i	-0.007	-0.007	0.003	0.004	0.004	0.003	0.002	0.000
$i+1$	-0.006	-0.006	0.004	0.005	0.004	0.004	0.002	-0.004
$i+2$	-0.005	-0.006	0.004	0.005	0.004	0.004	0.003	-0.003
$i+3$	-0.005	-0.006	0.004	0.005	0.004	0.004	0.003	-0.002
$i+4$	-0.005	-0.006	0.004	0.005	0.004	0.004	0.003	-0.002

reset of the rhythmic movement, with a reset magnitude of $-0.001s/rad$. All conditions but $C_{50\%}$ and $C_{43\%}$ generated a transient reset of the rhythmic movement before setting-up to the final reset value, during a variable duration between one and two oscillations. Conditions $C_{14\%}$, $C_{34\%}$ and $C_{83\%}$ showed a transient perturbation effect during two oscillations, whereas $C_{0\%}$, $C_{58\%}$ and $C_{95\%}$ induced a transient perturbation effect during one oscillation only. The maximum transient perturbation of the phase is observed under $C_{0\%}$ with a maximum magnitude of $-0.007s/rad$, $C_{14\%}$ of $-0.006s/rad$, and the least transient perturbation is observed under $C_{83\%}$ with a maximum transient phase reset magnitude of $0.002s/rad$. All the conditions but $C_{95\%}$ induced a perturbation during the oscillation i, compared to the oscillation $i+1$ for $C_{95\%}$.

Overall, both Fast and Slow conditions induced a phase reset of the rhythmic movement. Under both conditions, the condition that induced the greatest phase reset in magnitude is $C_{0\%}$, and $C_{14\%}$ under the Fast condition, with a maximum magnitude of $-0.007s/rad$, but $C_{14\%}$ in the Fast condition induces a final phase reset of $-0.006s$. Under both velocity conditions, three phase conditions induced a transient reset of the phase dur-

Table 3.6. Phase Reset in the Slow condition. Values in red show a positive shift of the phase with respect to the phase of a not-perturbed rhythmic movement -i.e. the rhythmic movement falls after the predicted value-. Values in blue show a negative shift of the phase of the rhythmic movement after the perturbation occurs -i.e. the rhythmic movement falls before the predicted value-. The values in yellow show the final constant reset of the phase after the recovery of the rhythmic limb from the perturbation.

	$C_{0\%}$	$C_{14\%}$	$C_{34\%}$	$C_{43\%}$	$C_{50\%}$	$C_{58\%}$	$C_{83\%}$	$C_{95\%}$
$i-1$	0.000	0.000	0.000	0.000	0.000	0.000	0.000	0.000
i	-0.007	-0.006	0.004	0.005	0.004	0.003	0.002	0.000
$i+1$	-0.005	-0.005	0.004	0.005	0.004	0.002	0.000	-0.004
$i+2$	-0.005	-0.004	0.005	0.005	0.004	0.002	0.001	-0.003
$i+3$	-0.005	-0.004	0.005	0.005	0.004	0.002	0.001	-0.003

ing two oscillations before stabilization of the phase reset to its final value, but under the Slow condition, $C_{43\%}$ and $C_{50\%}$ did not transiently perturbed the rhythmic condition since the phase reset reached directly its final value. There is then a dependence of the phase during which the perturbation occurs for the phase reset variable for both velocity conditions, but it is unclear whether one of the velocity condition has a greater effect on the rhythmic limb. The effect of the phase has to be taken into consideration rather than the effect of the velocity of the discrete movement. The main difference between the Fast and the Slow condition is about the duration of the phase reset. The Fast condition leads to a phase reset of two oscillations for four conditions out of eight whereas the Slow condition leads to a phase reset of two oscillations for all the eight conditions. This finding suggests that the Slow condition has a greater impact on the rhythmic movement, which is also supported by the maximum phase reset of $-0.09s$ under $C_{0\%}$ for the Slow condition, which is higher than the maximum phase reset of $-0.08s$ under $C_{0\%}$ for the Fast condition.

3.2. Co-contraction Results

Two sets of analyses were used to evaluate the role of co-contraction level in the change of the rhythmic movement. The first part of the current with evoke the results obtained of co-contraction levels, and the second part with evaluate the correlation between the co-contraction level during the initiation of the discrete movement and the associated phase shift.

3.2.1. Co-contraction level

Figures A.7, A.8 and Tables A.1, A.2 show the changes in the rhythmic co-contraction level after Fast and Slow discrete movement initiation. At the first sight, the results suggest that there were a differential effects of in the co-contraction levels for Flexion and Extension: with an overall increase of the co-contraction level for flexion, and a decrease during the extension. To avoid a misunderstanding of the results due to the transience in the co-contraction level results, Table 3.7 and 3.8 displays the results of the mean co-contraction levels subtracted from the baseline value between the flexion and the extension to evaluate the co-contraction level over the complete oscillation.

Results for the Fast condition suggest that the conditions that affected the rhythmic movement the most were $C_{0\%}$, $C_{14\%}$ and $C_{83\%}$, that shifts the co-contraction level from the baseline during three oscillations, closely followed by $C_{34\%}$, $C_{43\%}$, $C_{34\%}$ and $C_{95\%}$ that modulate the co-contraction level from baseline during two oscillations. For $C_{0\%}$, $C_{14\%}$, $C_{34\%}$, $C_{58\%}$ and $C_{83\%}$, the mean co-contraction decreased to -0.02, -0.20, -0.10, -0.03 and -0.06, respectively, before to increasing to a positive peak and returning to baseline. $C_{43\%}$, $C_{50\%}$ and $C_{95\%}$ all showed only a co-contraction level increase. $C_{14\%}$ was the condi-

tion under which the magnitude of the co-contraction is the highest, i.e. -0.20, and $C_{34\%}$ with a co-contraction level of -0.10 , whereas $C_{43\%}$, $C_{50\%}$ have a slight impact with an increase of 0.01 and 0.02 in the level of co-contraction. $C_{58\%}$ does not affect at all the co-contraction level that remains at the baseline. An interesting finding is that for $C_{50\%}$ to $C_{95\%}$, the co-contraction level increases only at the oscillation $i+1$, which differs from the other conditions that affects the co-contraction during he i^{st} oscillation.

Table 3.7. Mean flexion and extension co-contraction level under the fast condition, with subtraction of the co-contraction baseline value (i.e. mean flexion and extension co-contraction value before the perturbation occurs). Values in red show an increase of the co-contraction level whereas values in blue show a decrease in the co-contraction level.

	$C_{0\%}$	$C_{14\%}$	$C_{34\%}$	$C_{43\%}$	$C_{50\%}$	$C_{58\%}$	$C_{83\%}$	$C_{95\%}$
$i-1$	0.00	0.00	0.00	0.00	0.00	0.00	0.00	0.00
i	-0.02	-0.20	-0.10	0.01	0.00	-0.03	-0.06	0.00
$i+1$	0.03	0.03	0.01	0.01	0.02	0.03	0.07	0.04
$i+2$	0.01	0.01	0.00	0.00	0.00	0.00	0.01	0.02
$i+3$	0.00	0.00	0.00	0.00	0.00	0.00	0.00	0.00

For the Slow condition, the maximum decrease of co-contraction is observed under $C_{14\%}$ and $C_{34\%}$ with a magnitude of -0.23 and -0.12. Similarly to the Fast condition, the co-contraction level for $C_{95\%}$ is shifted from the baseline during the oscillation $i+1$,which differs from the other conditions that lead to an adaptation of the co-contraction during the i^{st} oscillation. All conditions lead to a decrease of the mean co-contraction level first, and showed then during the next oscillation a maximum peak of the co-contraction level before returning to the baseline value. $C_{43\%}$, $C_{58\%}$ and $C_{83\%}$ are shifting the co-contraction level from the baseline during four oscillations, which is larger than all the other conditions that shift the co-contraction level from the baseline during three oscillations.

Overall, the Slow condition had greater influence on the co-contraction level rather than the Fast condition, which was verified by the number of oscillations during which the

Table 3.8. Mean flexion and extension co-contraction level under the slow condition, with subtraction of the co-contraction baseline value (i.e. mean flexion and extension co-contraction value before the perturbation occurs). Values in red show an increase of the co-contraction level whereas values in blue show a decrease in the co-contraction level.

	$C_{0\%}$	$C_{14\%}$	$C_{34\%}$	$C_{43\%}$	$C_{50\%}$	$C_{58\%}$	$C_{83\%}$	$C_{95\%}$
$i-1$	0.00	0.00	0.00	0.00	0.00	0.00	0.00	0.00
i	-0.08	-0.23	-0.12	-0.01	-0.02	-0.04	-0.06	0.00
$i+1$	0.03	0.04	0.03	0.04	0.03	0.03	0.02	-0.02
$i+2$	0.01	0.01	0.01	0.01	0.01	0.01	0.02	0.02
$i+3$	0.00	0.00	0.00	0.01	0.00	0.01	0.01	0.01
$i+4$	0.00	0.00	0.00	0.00	0.00	0.00	0.00	0.00

co-contraction level was modulated from the baseline, and by the maximum absolute value of the co-contraction level highest under the Slow $C_{14\%}$ condition that decreases of 0.23.

3.2.2. Correlation between period shift and co-contraction level

Results of correlation between the period shifts and the co-contraction levels are presented in Figure 3.1. The results did not to show a co-variation of the two variables. The R-squared values reported on Figure 3.1 for both Fast and Slow conditions together, as well as separated are equal to 0.08, which shows a very low correlation between the two variables.

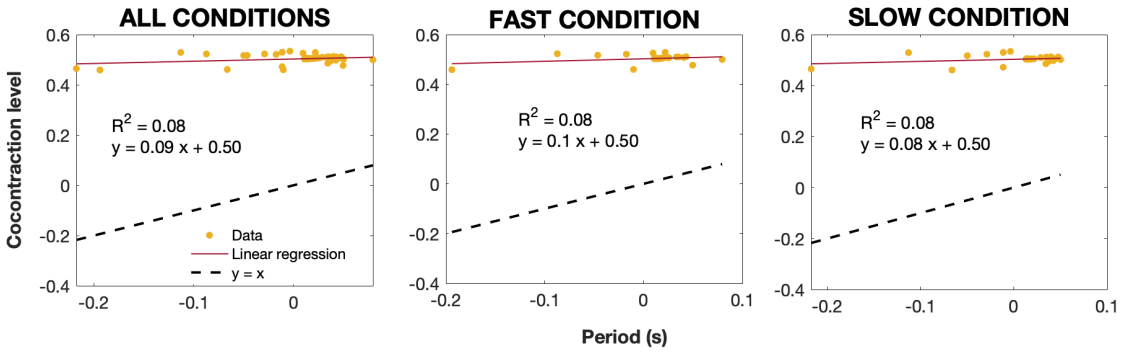

Figure 3.1. Correlation between the co-contraction level and period shift for all the data, for the Fast condition, and for the Slow condition. The black dashed line represent the y=x line, the each point in the orange point cloud represent the measure of the co-contraction level in function of the period shift within one oscillation, and the red line corresponds to the best fitted line to the point cloud data. R^2 measure and equation of the best fitted line have been reported.

Chapter 4. Discussion

Two hypotheses about the source of interference between rhythmic and discrete movements were tested in this study. First, we hypothesized that the magnitude of interference between these movement types depends on the velocity discrepancy between the rhythmic and the discrete movement. Second, we tested the extent to which decreases in the period of rhythmic movement following discrete response initiation relate to changes in the co-contraction levels of the rhythmic limb.

The results suggested that the adaptation of the rhythmic movement to the discrete perturbation is not directly linked to the velocity of the discrete movement. Fast and Slow discrete movements were stimulated to have peak angular velocity 20% higher or lower than the peak angular velocity of the rhythmic movement, respectively. There were no major differences between the two conditions in term of period shift in the rhythmic oscillations in response of the rhythmic movement. Nevertheless, it was observed that the behavioral response of the rhythmic movement was dependent on the phase of the rhythmic movement during which the perturbation occurred. A slightly longer return of the rhythmic movement's period for $C_{50\%}$ and $C_{83\%}$ under the Fast condition suggest that the rhythmic movement undergoes a greater perturbation than in the the Slow condition if the discrete movement is initiated at those specific phases.

Differences were observed with respect to the phase of the rhythmic movement during which the discrete movement was initiated. Those differences likely stem from the symmetry in the activation of the agonist and antagonist muscles groups of the rhythmic and discrete limbs. Indeed, when the two limbs are performing a flexion, the magnitude of the phase reset is lower than when the movements are performed in an opposite direc-

tion. Similar findings were previously reported by Kennedy et al. for the discrete movement reaction time during bimanual movements involving rhythmic-discrete coordination task – faster reaction times were observed when both limbs moved activated homologous muscle groups (flexion-flexion, extension-extension) and slower when they moved in different ways (flexion-extension) [24]. There are two main explanations commonly discussed to describe this observed behavior. The first one, referenced to as the egocentric frame of reference [42], suggests that there is neuronal cross-talk when non-homologous muscles groups are simultaneously activated, creating a higher interference between the two limbs, i.e. a greater perturbation of the rhythmic movement's phase [72]. The second main explanation for a phase reset to happen, known as the allocentric frame of reference [42], relates to the impact on the motor behavior of two limbs moving in a similar direction in space, which has been reported to be a more stable condition rather than when the limbs are moving in a different directions. Further experiments are needed to determine whether the cross-talk or the directional effects are most likely to be observed when preforming the bimanual rhythmic/discrete task described here. One way to verify the impact of both allocentric and egocentric frame of reference would be to perform the same task as presented here, but to change the direction of the discrete movement so that the homologous muscles would be activated in a different phase of the rhythmic movement. Empirical results have previously reported behavioral response of the rhythmic arm after a perturbation was induced by a discrete movement. It remains not clear whether a rhythmic arm has a tendency to speed up or to slow down on a response to a discrete movement from a contralateral arm. The current study may bring some elements of answers suggesting that the behavior or the rhythmic movement would actually depend on the phase of the rhythmic

movement during which the perturbation occurs.

Another explanation that may account for observing a majority of slow-down rather than some speed-ups of the rhythmic movement might be the fast initial frequency of the rhythmic movement. The rhythmic movement is initially at 2Hz, which is a movement already very fast for an oscillatory behavior around the elbow. The arms' inertia is taken into account in the model for the definition of each limb, so the maximum speed at which the model can perform the rhythmic movement may be limited. An adaptation of the model to a rhythmic movement with different properties would give further insights on this.

Furthermore, findings on the shift in amplitude of the rhythmic movement when the discrete movement occurs also report that the amplitude shift is dependent on the phase on the rhythmic movement during which the discrete movement is performed. The results did not show a single behavioral response of the rhythmic movement regarding the amplitude shift, but rather showed different responses depending on the phase condition. For this dependent measure as well, the Slow condition had a greater impact on the rhythmic movement since the amplitude overall took more oscillations to get back to its baseline value. To elaborate on the independent variables responsible of modifying the rhythmic movement's amplitude and quantify the modifications of the rhythmic behavior, more experiments have to be conducted. One could wonder to what extent the interference between bimanual rhythmic/discrete depends on the amplitude of the discrete movement, i.e. if a discrete movement of amplitude shorter than the amplitude of the rhythmic movement leads to a smaller shift in amplitude of the rhythmic movement compared to a discrete movement with an amplitude larger than the rhythmic movement's one.

The results of empirical research suggest that there is not a single response that has been observed in a rhythmic movement when being perturbed by a discrete movement. The work presented may introduce an element of answer for such different behaviors observed since it was observed that the response of the rhythmic movement is generally dependent on the phase of the rhythmic movement during which the discrete movement occurs – which needs to be taken into consideration in analyzing bimanual rhythmic/discrete interference produced by human participants.

The second hypothesis was tested by examining the co-contraction level of the rhythmic movement following initiation of the discrete response. The co-contraction was defined as the overlap between the firing rates the rhythmic arm's antagonist/agonist neurons throughout the movement cycle. One major finding related to the co-contraction level is that the Slow condition was more challenging to adapt to, so that the co-contraction level was modulated from baseline value during a greater number of oscillations under the Slow condition compared to the Fast condition, but it has not been confirmed that there exist a co-variation of the oscillation's period and the co-contraction level. Nevertheless, for both velocity conditions, and under almost all the conditions on the phases of initiation of the discrete movement, the co-contraction level decreased at the oscillation i during which the perturbation occurred, and increased in the next oscillations before the value returns to the baseline. It is still unclear whether an decrease in co-contraction level is a redundant finding while a perturbation occurs during a motor task, and it appears that different compensation techniques can be adopted by different groups of population when trying to adapt to a perturbation. The findings of this study are solely based on a simulation that may not best relate to the physiological adaptation mechanisms that occur in

humans, and further experiments would need to be conducted in order to drive conclusions on this matter.

Previously reported results by Lohse et al. suggest that an external focus of attention reduces the co-contraction level of agonist and antagonist muscles groups compared to an internal frame of attention [73]. The results of this simulation study did not allow to draw conclusions on whether the cross-talk or allocentric frame of reference was a correct explanation for the rhythmic behavior observed when perturbed by a discrete movement. It is possible that directing the attention externally from the rhythmic limb to the contralateral limb (to initiate the discrete response) contributed to the decrease in the co-contraction level of the rhythmic limb.

Chapter 5. Conclusion

This simulation study did not support the hypothesis that the magnitude of interference of rhythmic and discrete movements depends on their the velocity congruence. This hypothesis was tested using simulations from the model proposed by Ronsse et al. [1] adapted to a bimanual rhythmic discrete task. The second hypothesis was to test whether the decrease in the rhythmic arm oscillation period is correlated to an increase in the co-contraction level of the rhythmic limb. This hypothesis was also not supported because no co-variation patterns were observed between the two variables. Further work would be necessary to test the accuracy of the predictions from this simulation study using experimental data.

Chapter 6. Limitations of the study

In this study, with using the Matusoka Oscillator model presented by [1], I was able to successfully evaluate the hypothesis about the effects of velocity congruency between a bimanual rhythmic/discrete movements. Nevertheless, the usage of the model has led to difficulties, that forced an adaptation of the task based on the model's characteristics.

Indeed, a more extensive definition of each of the parameters used in the model would have been very helpful to fully understand the physiological meaning of the adaptation of one or more parameters. Attempts have been made to simulate the movements presented in the study so that the amplitude of the rhythmic and the discrete movements would be the same, but a failure happened in the simulation of the discrete movement when modifying the temporal parameters as suggested in the original publication. One thought is that the modification of the temporal parameters of the model is possible only when adaption all the other simulation parameters to those newly defined parameters. One attempt has also been made to adapt the parameters of the limb performing the rhythmic movement only, but a default was observed in the discrete movement as well. Creating an asymmetry in the simulation parameters between the two limbs seems to be a reasonable change to the model since evidences exist that not a single CPG structure is responsible for the upper-limb rhythmic movement generation, and other studies suggest that each joint structured by an agonist/antagonist set of muscles might be governed by an own CPG center [74, 75, 35]. Furthermore, the parameters of the model are the same for the definition of each movement type, but are also the same in the coupling terms. No specific parameters have been reported in this model to differentiate between bimanual rhythmic/rhythmic coupling, or bimanual rhythmic/rhythmic coupling. The coupling

assessed with the model is based on the feedback given from each limb to the contralateral one, but no terms of neural command coupling has been defined in the model. If only looking at the bimanual motor activities in a population that has undergone a stroke, there is a huge degradation of the bimanual capabilities [76], and many studies have previously demonstrated the interaction, i.e. cross-talk effects during bimanual activities [72, 77]. One can wonder to what extent the outcomes of a simplified model can be used to drive conclusions on a population, and whether the lack of consideration of many physiological behaviors in the model is reasonable or not.

More information on the other specifications such as the limitation of the model would have been helpful to design a more precise simulation. As determined through experimental testing, some low values of discrete movement's duration fail to generate a well-shaped discrete movement, inducing the limb to systematically overshoot or undershoot the predefined reference value $\theta^\star$ of the discrete movement. Those failure from the model were considered to be limitations of the model, but one could be unsure whether the failure comes from the model limitation, or if it would come from a mistake in the reproduction of the model. The reproduction of the model requires the investigator to have an extended knowledge of technical software such as Simulink (MathWorks, Natik, MA), and a thorough understanding of systems of differential equations. One way to overcome this reproduction matter would be to enhance the usage of a sharing platform on which models or validation results could be shared to all researchers in the field [1].

Using the Matusoka oscillator proposed by Ronsse et al has been helpful, and has required to make some explicit assumptions regarding the underlying mechanisms producing discrete and rhythmic movements, as well as the coupling involved between the two

limbs. First, all the parameters used to define the model are the same for both types of movement, with the only exception of the shape of the input signal fed to the rhythmic and the discrete CPGs. The CPG model is originally developed for rhythmic movements, but the adaptation of the model to the discrete movement suggests that in this case, the discrete movement is simply a truncated rhythmic movement that requires a more complicated input function. The complication that arose in the definition of the discrete movement's input signal could be related to the activation of additional brain regions to generate a discrete movement, compared to a rhythmic one, if it is considered that this additional brain activation is solely related to the generation of a discrete movement.

Chapter 7. Future Directions

Future work should test the model predictions described in this thesis using experimental data from human participants. The collection of EMG signals as well as kinematic data from upper limbs during the performance of this bimanual rhythmic/discrete interaction task would allow for a better estimation of the co-contraction level of each antagonist muscle of the rhythmic arm, and kinematic data would allow to quantify the influence of the discrete movement on the rhythmic one.

A second idea could be to generate a discrete movement in a direction opposite of the direction presented in this study. As for now, it was considered that the discrete movement is a flexion, and to further evaluate the egocentric and allocentric assumptions discussed in Chapter 4, generating an extension discrete movement could give some interesting insights.

Furthermore, if the velocity of the discrete movement did not appear to have an influence on the response of the rhythmic movement, it must be interesting to evaluate the influence of the amplitude of the discrete movement on the response of the rhythmic movement.

The use of the CPG model to generate discrete movements has not been biologically verified. Many studies have assessed the generation of rhythmic movements in transected animal under a constant stimulation of the concerned limbs, but none of the studies assessed the capability of CPG circuits to generate discrete movements under the influence of a specially-shaped input.

Appendix A. Additional Results

Table A.1. co-contraction level under fast condition. Values in red show an increase of the co-contraction level whereas values in blue show a decrease of the co-contraction level.

	$C_{0\%}$	$C_{14\%}$	$C_{34\%}$	$C_{43\%}$	$C_{50\%}$	$C_{58\%}$	$C_{83\%}$	$C_{95\%}$
$(i-1)_F$	0.70	0.71	0.71	0.71	0.71	0.71	0.59	0.61
$(i-1)_E$	0.70	0.71	0.71	0.71	0.71	0.71	0.60	0.61
i_F	0.82	0.43	0.48	0.71	0.71	0.71	0.59	0.61
i_E	0.53	0.57	0.73	0.72	0.70	0.64	0.48	0.61
$(i+1)_F$	0.79	0.77	0.72	0.72	0.74	0.77	0.82	0.82
$(i+1)_E$	0.67	0.69	0.70	0.70	0.70	0.69	0.50	0.48
$(i+2)_F$	0.71	0.71	0.71	0.71	0.71	0.71	0.63	0.68
$(i+2)_E$	0.70	0.71	0.70	0.70	0.70	0.70	0.58	0.59
$(i+3)_F$	0.70	0.71	0.71	0.71	0.71	0.71	0.60	0.62
$(i+3)_E$	0.70	0.71	0.70	0.70	0.70	0.70	0.59	0.61
$(i+4)_F$	0.70	0.71	0.71	0.71	0.71	0.71	0.60	0.61
$(i+4)_E$	0.70	0.71	0.70	0.70	0.70	0.70	0.59	0.61

Table A.2. co-contraction level under slow condition. Values in red show an increase of the co-contraction level whereas values in blue show a decrease of the co-contraction level.

	$C_{0\%}$	$C_{14\%}$	$C_{34\%}$	$C_{43\%}$	$C_{50\%}$	$C_{58\%}$	$C_{83\%}$	$C_{95\%}$
$(i-1)_F$	0.70	0.70	0.70	0.70	0.70	0.69	0.64	0.69
$(i-1)_E$	0.70	0.70	0.71	0.71	0.70	0.69	0.64	0.69
i_F	0.75	0.42	0.48	0.71	0.70	0.69	0.64	0.69
i_E	0.50	0.53	0.67	0.67	0.65	0.61	0.52	0.69
$(i+1)_F$	0.79	0.81	0.80	0.82	0.82	0.82	0.82	0.82
$(i+1)_E$	0.66	0.67	0.67	0.66	0.63	0.61	0.50	0.51
$(i+2)_F$	0.72	0.72	0.72	0.72	0.72	0.72	0.69	0.76
$(i+2)_E$	0.70	0.70	0.70	0.70	0.69	0.67	0.62	0.65
$(i+3)_F$	0.71	0.71	0.71	0.71	0.70	0.69	0.65	0.70
$(i+3)_E$	0.70	0.70	0.70	0.70	0.70	0.69	0.64	0.68
$(i+4)_F$	0.70	0.70	0.71	0.71	0.69	0.69	0.64	0.69
$(i+4)_E$	0.70	0.70	0.70	0.71	0.70	0.69	0.64	0.69

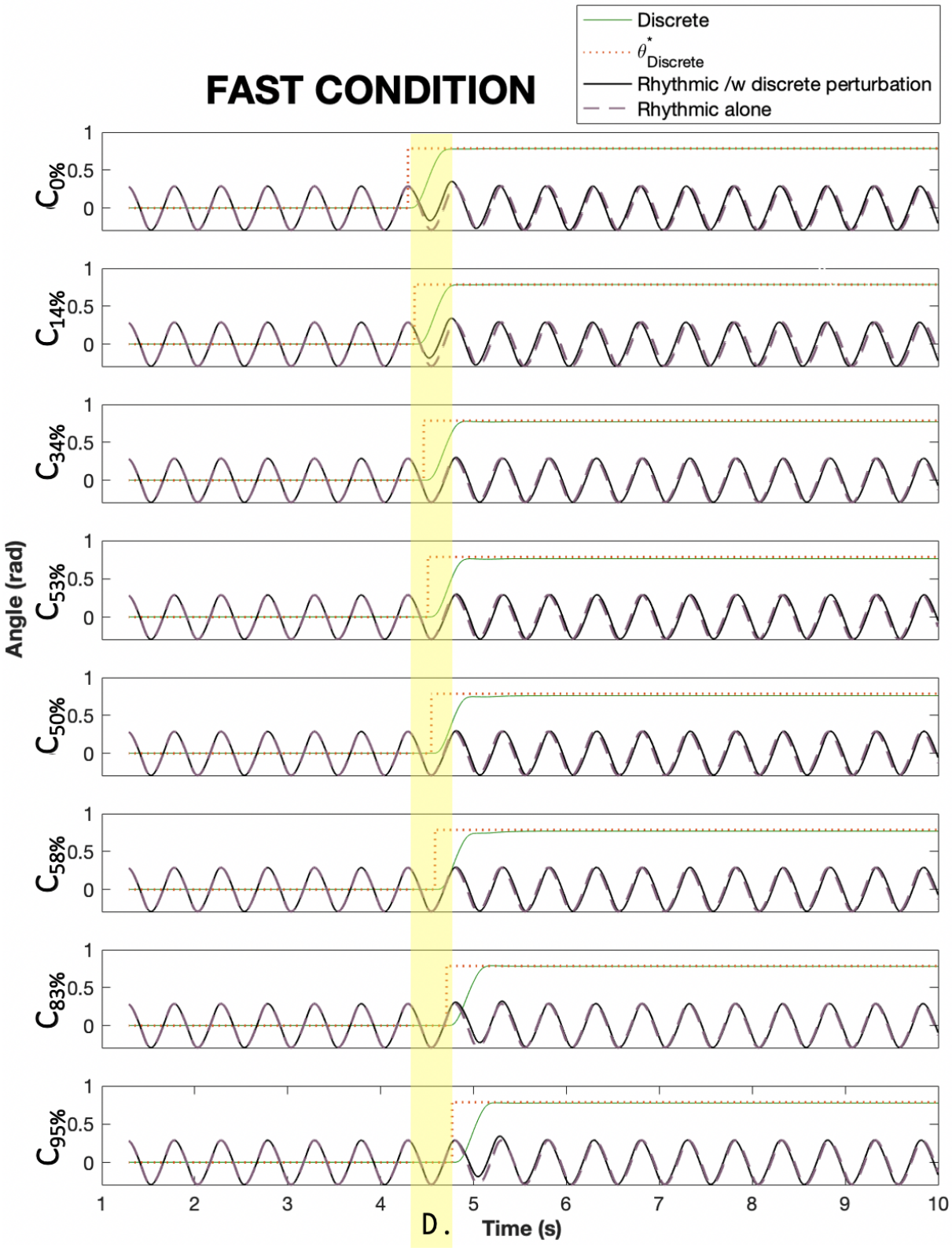

Figure A.1. Discrete and rhythmic movements in radian under each Fast conditions

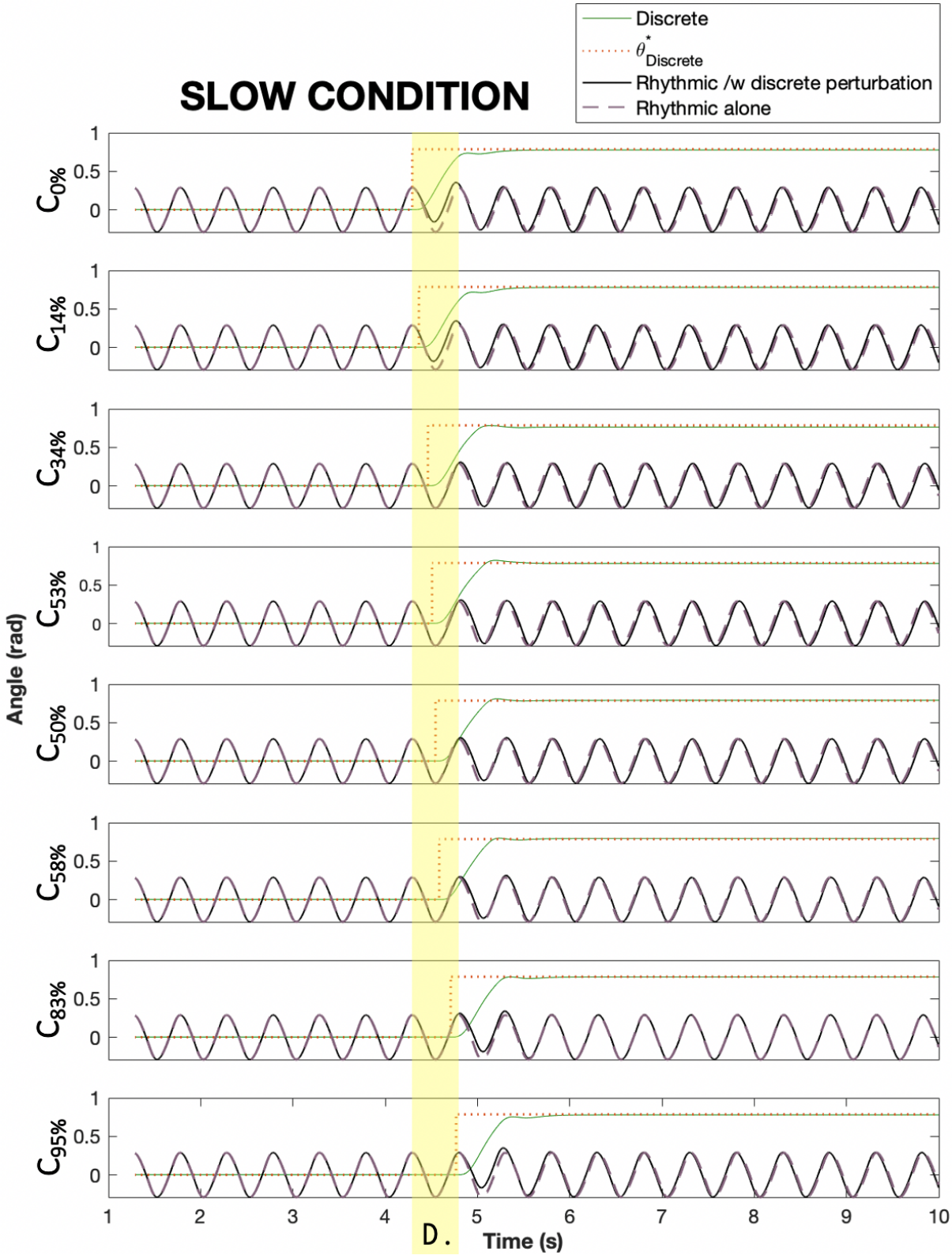

Figure A.2. Discrete and rhythmic movements in radian under each Slow conditions

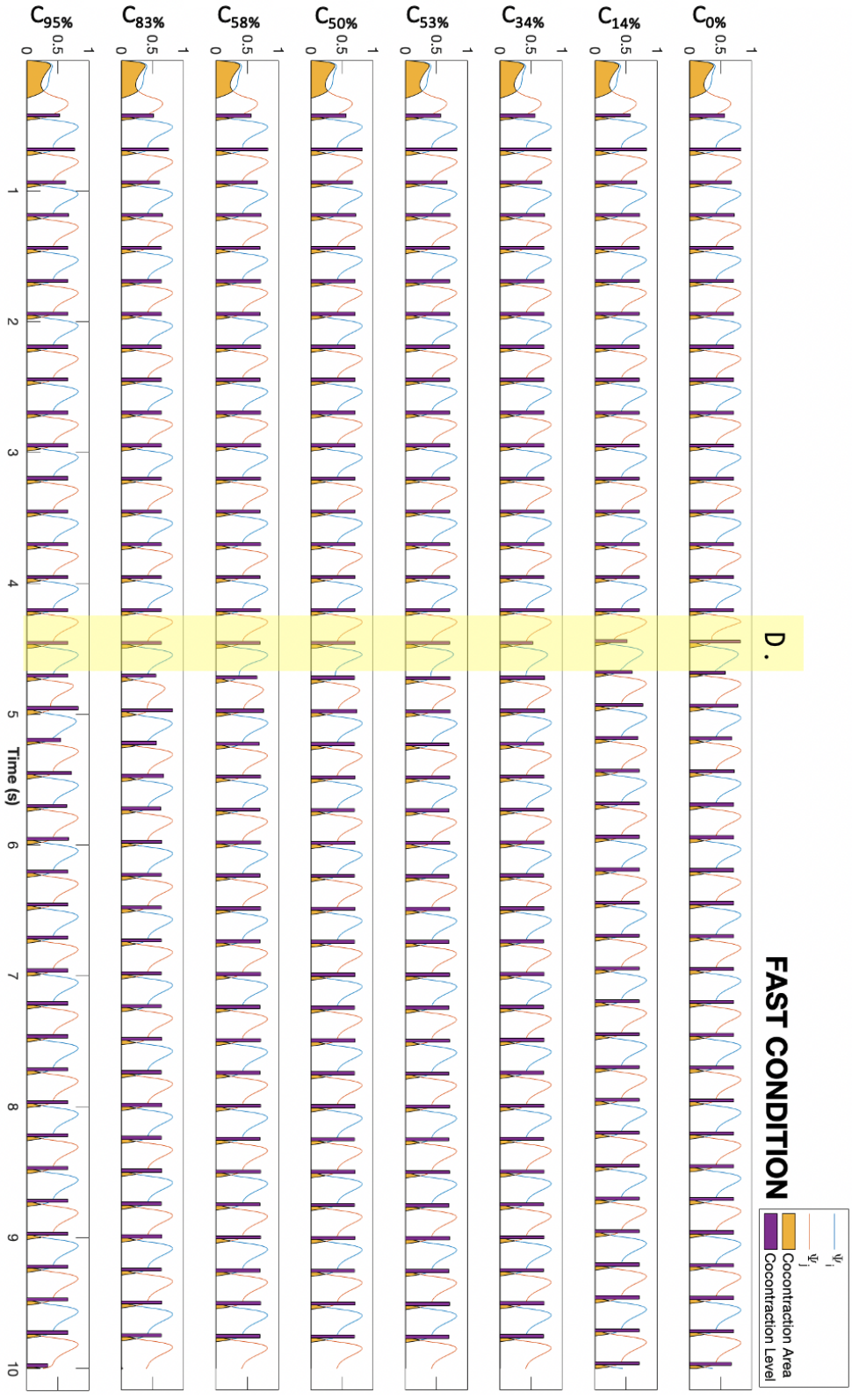

Figure A.3. Cocontraction levels under each Slow conditions

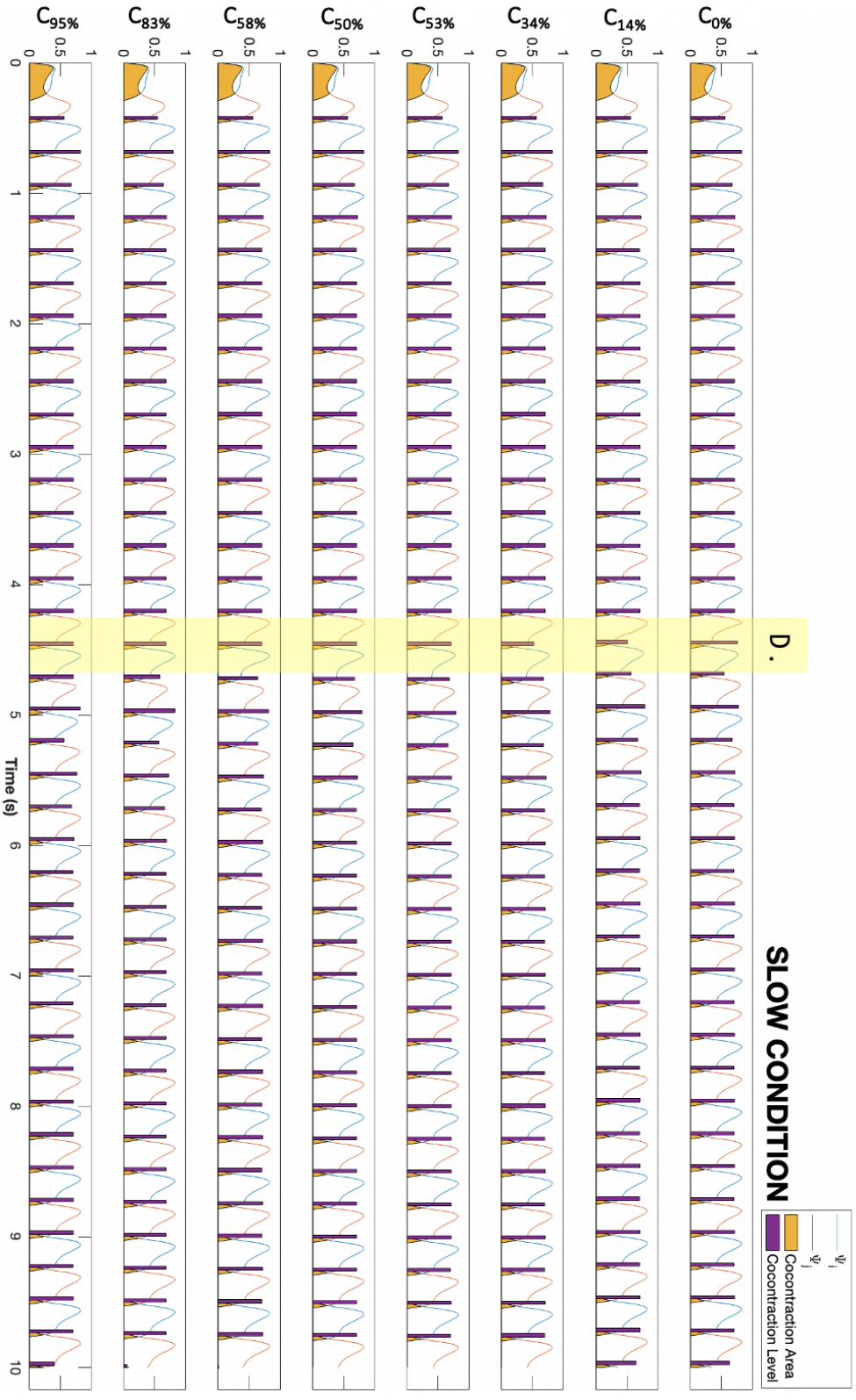

Figure A.4. Cocontraction levels under each Fast conditions

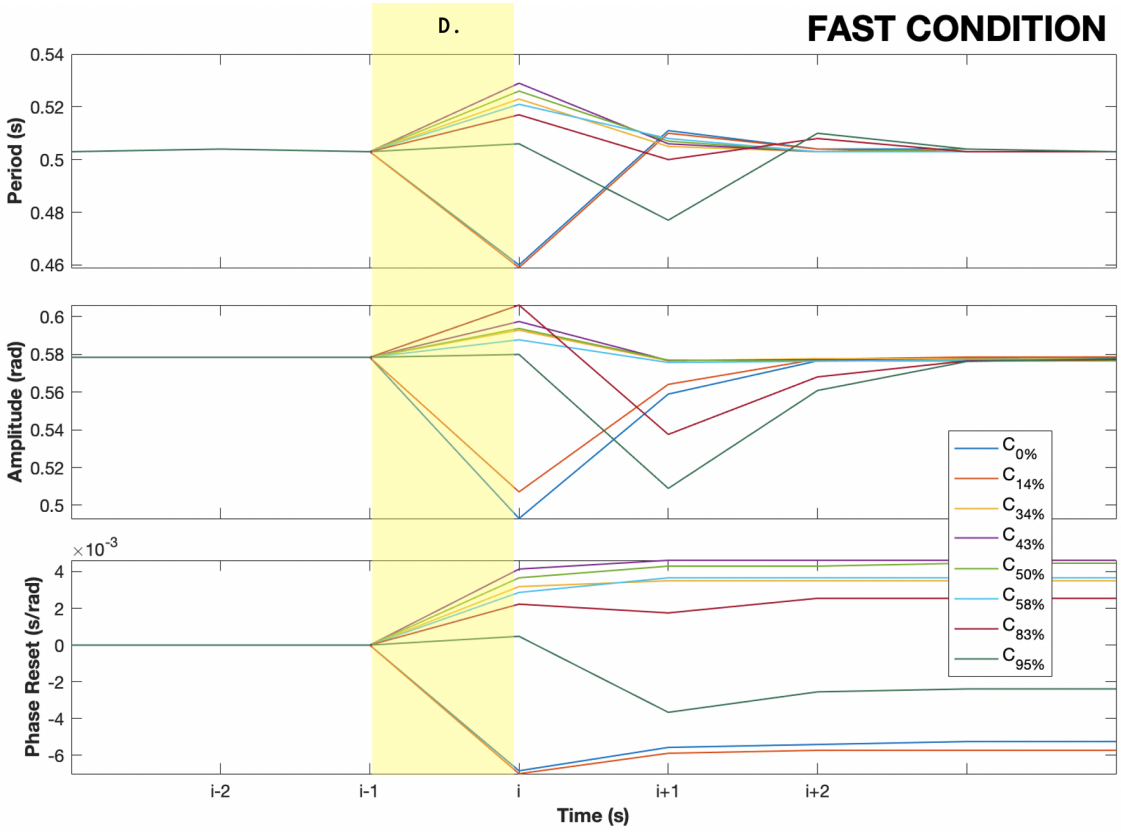

Figure A.5. Visual representation of the three dependent variables over time under the eight phase condition, for a rhythmic movement under the influence of a fast discrete movement. The area in yellow represents the time during which the discrete ($D.$) movement occurs. The indexing allows to refer to Tables 3.1, 3.5, 3.3

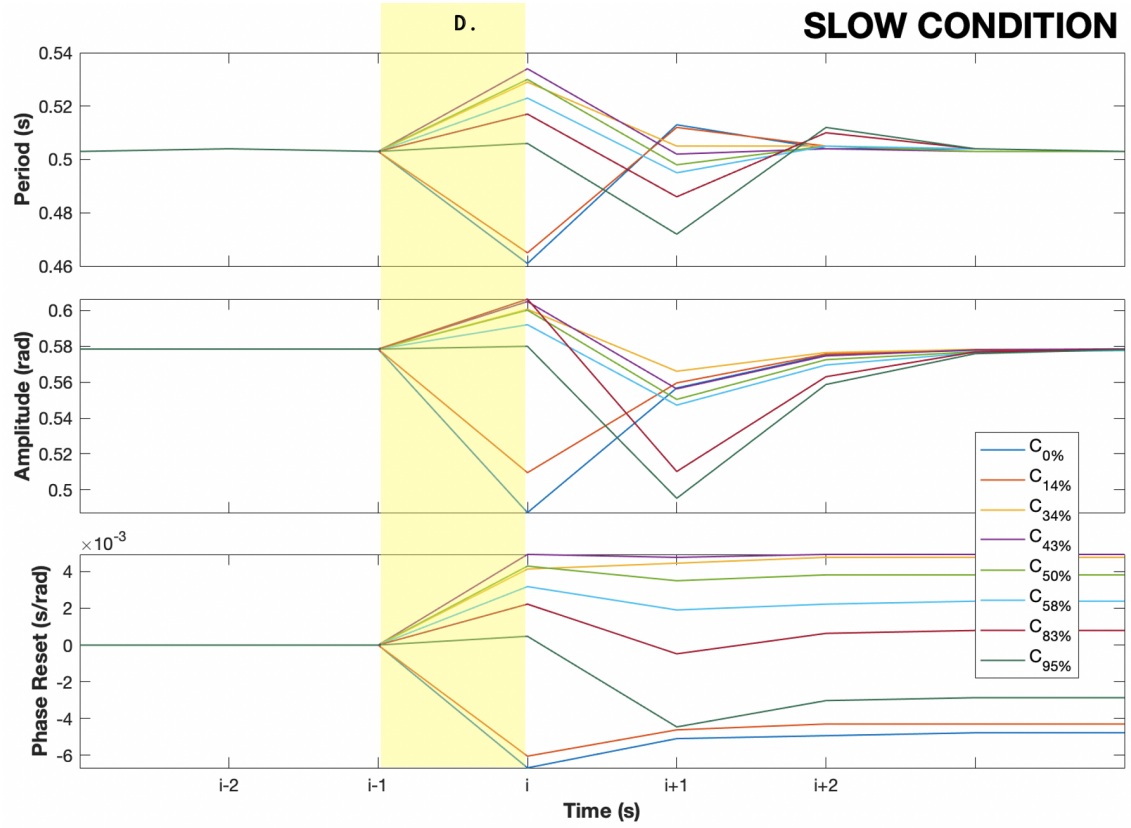

Figure A.6. Visual representation of the three dependent variables over time under the eight phase condition, for a rhythmic movement under the influence of a slow discrete movement. The area in yellow represents the time during which the discrete ($D.$) movement occurs. The indexing allows to refer to Tables 3.2, 3.4, 3.6,

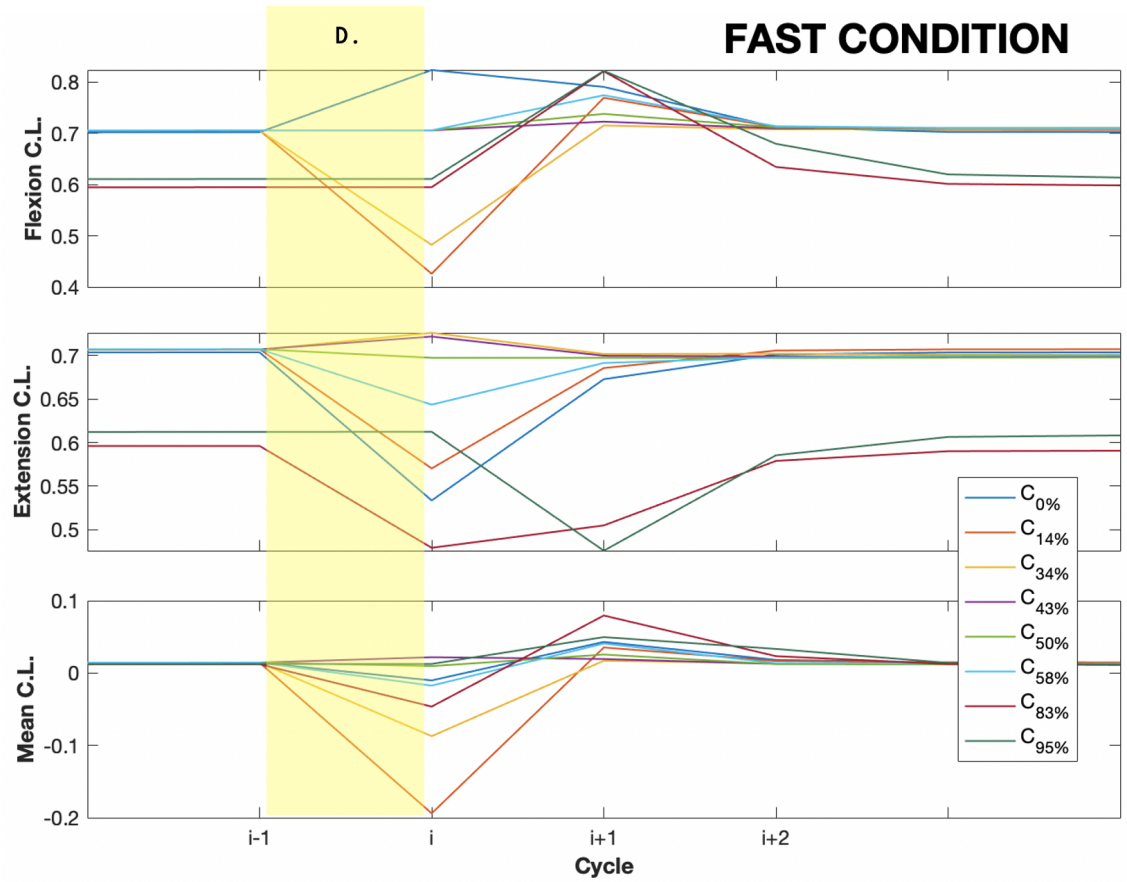

Figure A.7. Co-contraction level (C.L.) under the fast (first graph) for each of the eight phase condition of the initiation of the discrete movement. The first graph shows the C.L. during flexion, the second graph during extension, and the third graph shows the mean C.L. over flexion and extension.The indexing allows to refer to Table A.1 for more detailed results. The yellow area corresponds to the time during which the discrete movement ($D.$) occurs.

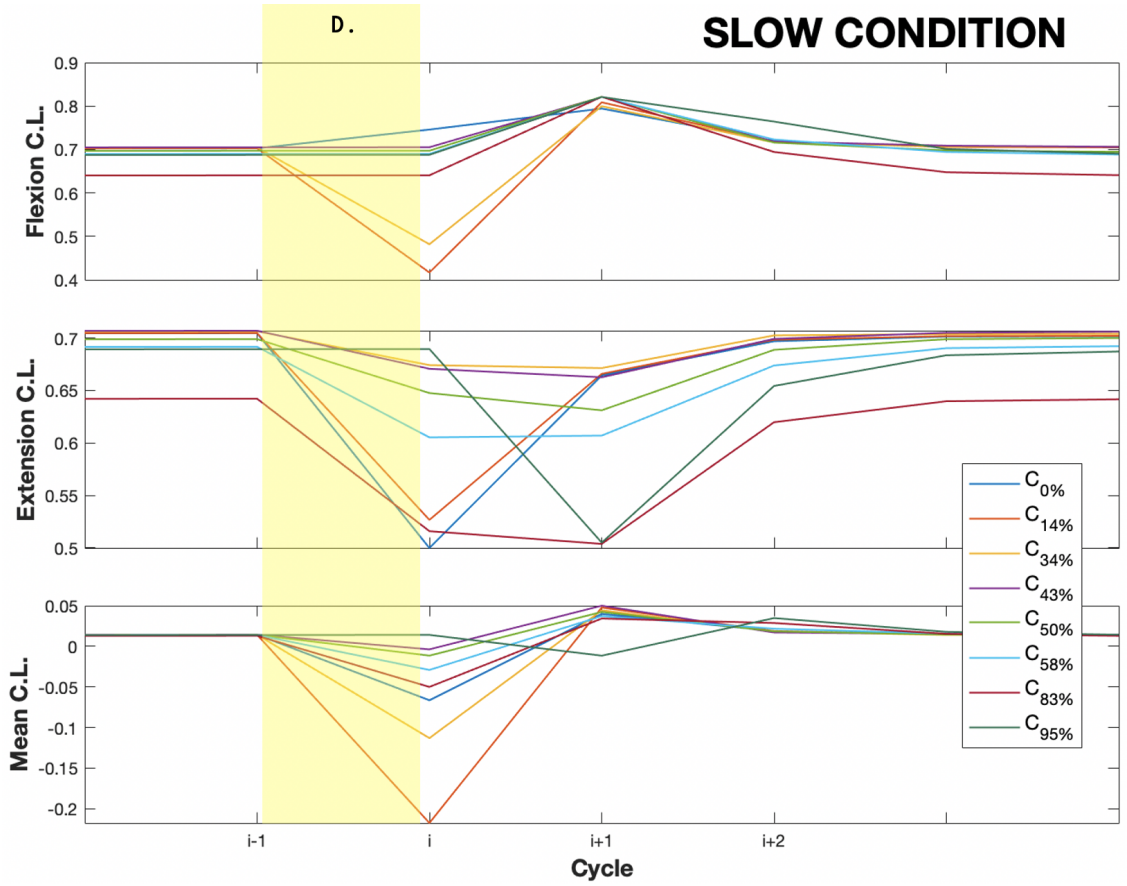

Figure A.8. Co-contraction level (C.L.) under the fast (first graph) and slow condition (second graph), for each of the eight phase condition of the initiation of the discrete movement. The indexing allows to refer to Table A.2 for more detailed results. The yellow area corresponds to the time during which the discrete movement ($D.$) occurs.

Appendix B. Simulation Diagrams

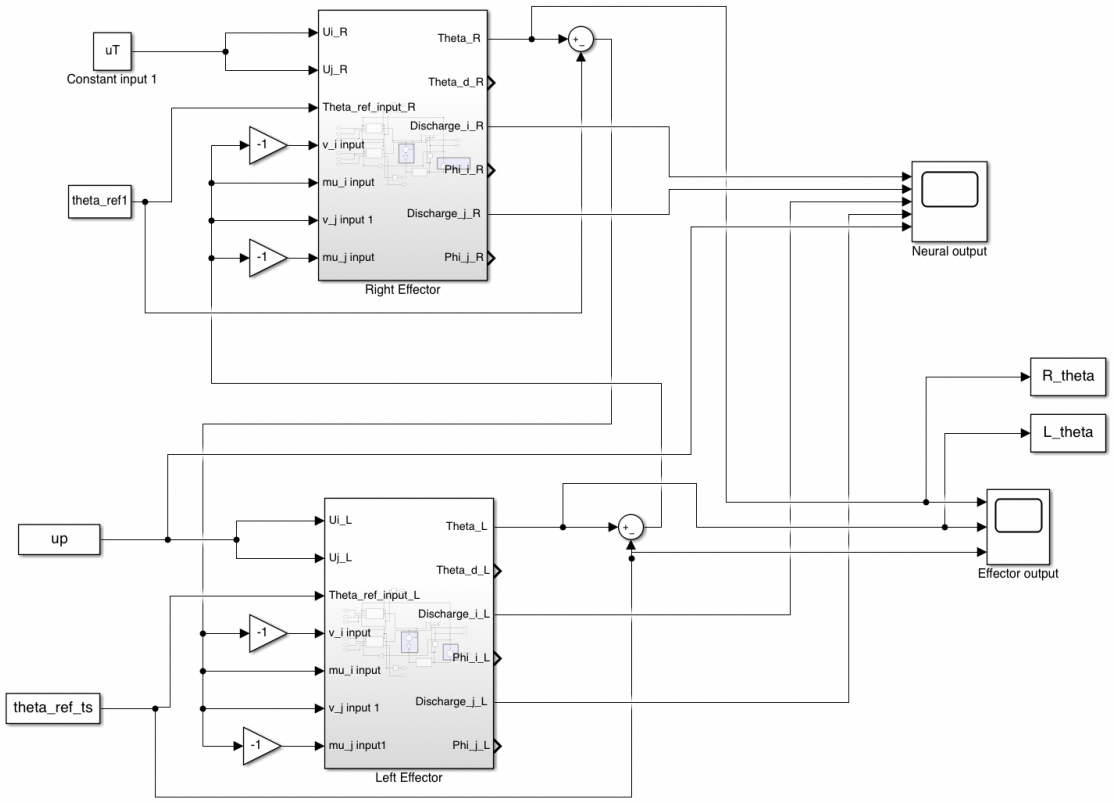

Figure B.1. Simulink: General diagram showing both limbs coupling

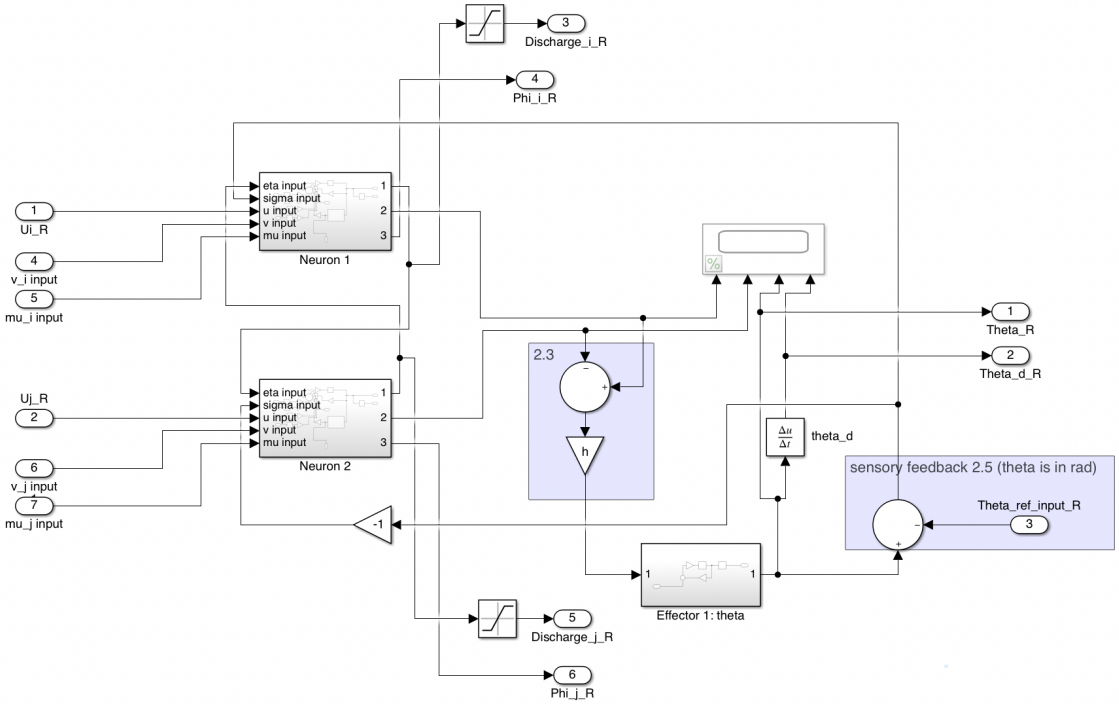

Figure B.2. Simulink: Diagram of the right effector.

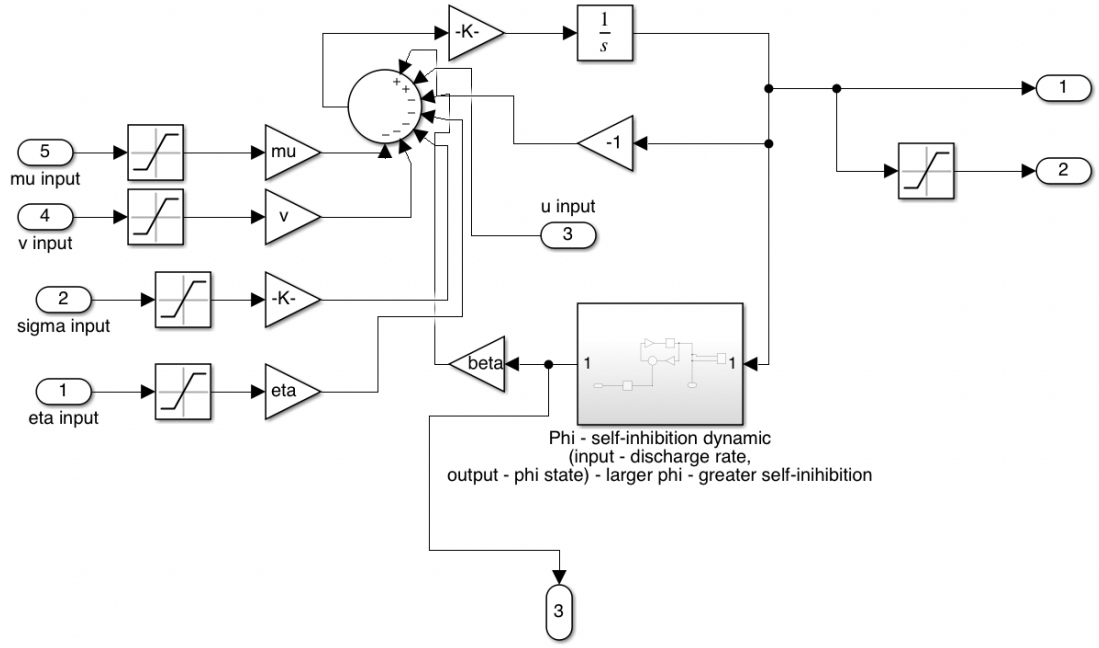

Figure B.3. Simulink: Diagram of the first neuron of the right effector

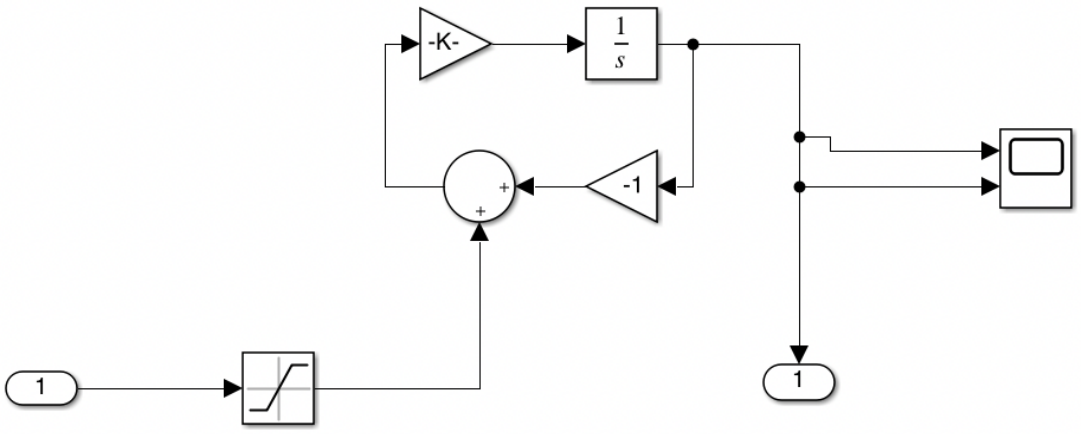

Figure B.4. Simulink: Diagram of the self-inhibition term of the right effector's first neuron.

Bibliography

[1] R. Ronsse, D. Sternad, and P. Lefevre, "A computational model for rhythmic and discrete movements in uni-and bimanual coordination," *Neural computation*, vol. 21, no. 5, pp. 1335–1370, 2009.

[2] H. Haken, J. S. Kelso, and H. Bunz, "A theoretical model of phase transitions in human hand movements," *Biological cybernetics*, vol. 51, no. 5, pp. 347–356, 1985.

[3] S. P. Swinnen, N. Dounskaia, C. B. Walter, and D. J. Serrien, "Preferred and induced coordination modes during the acquisition of bimanual movements with a 2: 1 frequency ratio." *Journal of Experimental Psychology: Human perception and performance*, vol. 23, no. 4, p. 1087, 1997.

[4] S. Calvin, R. Huys, and V. K. Jirsa, "Interference effects in bimanual coordination are independent of movement type." *Journal of Experimental Psychology: Human Perception and Performance*, vol. 36, no. 6, p. 1553, 2010.

[5] N. Hogan and D. Sternad, "On rhythmic and discrete movements: reflections, definitions and implications for motor control," *Experimental Brain Research*, vol. 181, no. 1, pp. 13–30, 2007.

[6] T. Ikegami, M. Hirashima, G. Taga, and D. Nozaki, "Asymmetric transfer of visuomotor learning between discrete and rhythmic movements," *Journal of Neuroscience*, vol. 30, no. 12, pp. 4515–4521, 2010.

[7] R. C. Miall and R. Ivry, "Moving to a different beat," *Nature neuroscience*, vol. 7, no. 10, pp. 1025–1026, 2004.

[8] S. Schaal, D. Sternad, R. Osu, and M. Kawato, "Rhythmic arm movement is not discrete," *Nature neuroscience*, vol. 7, no. 10, pp. 1136–1143, 2004.

[9] J. J. Buchanan, J.-H. Park, and C. H. Shea, "Target width scaling in a repetitive aiming task: switching between cyclical and discrete units of action," *Experimental Brain Research*, vol. 175, no. 4, pp. 710–725, 2006.

[10] D. Sternad, "Debates in dynamics: a dynamical systems perspective on action and perception," 2000.

[11] D. Sternad and W. J. Dean, "Rhythmic and discrete elements in multi-joint coordination," *Brain research*, vol. 989, no. 2, pp. 152–171, 2003.

[12] A. M. van Mourik and P. J. Beek, "Discrete and cyclical movements: unified dynamics or separate control?" *Acta psychologica*, vol. 117, no. 2, pp. 121–138, 2004.

[13] I. S. Howard, J. N. Ingram, and D. M. Wolpert, "Separate representations of dynamics in rhythmic and discrete movements: evidence from motor learning," *Journal of Neurophysiology*, vol. 105, no. 4, pp. 1722–1731, 2011.

[14] J. A. Adams, "Historical review and appraisal of research on the learning, retention, and transfer of human motor skills." *Psychological bulletin*, vol. 101, no. 1, p. 41, 1987.

[15] H. Heuer, "Intermanual interactions during simultaneous execution and programming of finger movements," *Journal of Motor Behavior*, vol. 17, no. 3, pp. 335–354, 1985.

[16] J. S. Kelso, *Dynamic patterns: The self-organization of brain and behavior*. MIT press, 1995.

[17] K. Wei, G. Wertman, and D. Sternad, "Interactions between rhythmic and discrete components in a bimanual task," *Motor Control*, vol. 7, no. 2, pp. 134–154, 2003.

[18] S. P. Swinnen, N. Dounskaia, O. Levin, and J. Duysens, "Constraints during bimanual coordination: the role of direction in relation to amplitude and force requirements," *Behavioural Brain Research*, vol. 123, no. 2, pp. 201–218, 2001.

[19] J. S. Kelso, D. L. Southard, and D. Goodman, "On the coordination of two-handed movements." *Journal of Experimental Psychology: Human Perception and Performance*, vol. 5, no. 2, p. 229, 1979.

[20] J. J. Summers, J. A. Todd, and Y. H. Kim, "The influence of perceptual and motor factors on bimanual coordination in a polyrhythmic tapping task," *Psychological Research*, vol. 55, no. 2, pp. 107–115, 1993.

[21] M. L. Latash and V. M. Zatsiorsky, "Joint stiffness: Myth or reality?" *Human movement science*, vol. 12, no. 6, pp. 653–692, 1993.

[22] E. Burdet, R. Osu, D. W. Franklin, T. E. Milner, and M. Kawato, "The central nervous system stabilizes unstable dynamics by learning optimal impedance," *Nature*, vol. 414, no. 6862, pp. 446–449, 2001.

[23] D. Cattaert, A. Semjen, and J. Summers, "Simulating a neural cross-talk model for between-hand interference during bimanual circle drawing," *Biological Cybernetics*, vol. 81, no. 4, pp. 343–358, 1999.

[24] D. M. Kennedy, C. Wang, and C. H. Shea, "Reacting while moving: influence of right limb movement on left limb reaction," *Experimental brain research*, vol. 230, no. 1, pp. 143–152, 2013.

[25] S. P. Swinnen, N. Dounskaia, and J. Duysens, "Patterns of bimanual interference re-

veal movement encoding within a radial egocentric reference frame," *Journal of cognitive neuroscience*, vol. 14, no. 3, pp. 463–471, 2002.

[26] J. Kelso, "Phase transitions and critical behavior in human bimanual coordination," *American Journal of Physiology-Regulatory, Integrative and Comparative Physiology*, vol. 246, no. 6, pp. R1000–R1004, 1984.

[27] W. D. Byblow, D. Bysouth-Young, J. J. Summers, and R. G. Carson, "Performance asymmetries and coupling dynamics in the acquisition of multifrequency bimanual coordination," *Psychological Research*, vol. 61, no. 1, pp. 56–70, 1998.

[28] W. D. Byblow and D. Goodman, "Performance asymmetries in multifrequency coordination," *Human Movement Science*, vol. 13, no. 2, pp. 147–174, 1994.

[29] V. Puttemans, N. Wenderoth, and S. P. Swinnen, "Changes in brain activation during the acquisition of a multifrequency bimanual coordination task: from the cognitive stage to advanced levels of automaticity," *Journal of Neuroscience*, vol. 25, no. 17, pp. 4270–4278, 2005.

[30] S. C. de Oliveira, "The neuronal basis of bimanual coordination: recent neurophysiological evidence and functional models," *Acta psychologica*, vol. 110, no. 2-3, pp. 139–159, 2002.

[31] A. H. Cohen, S. Rossignol, S. Grillner *et al.*, *Neural control of rhythmic movements in vertebrates*. Wiley, 1988.

[32] J. J. Collins and S. A. Richmond, "Hard-wired central pattern generators for quadrupedal locomotion," *Biological Cybernetics*, vol. 71, no. 5, pp. 375–385, 1994.

[33] M. R. Dimitrijevic, Y. Gerasimenko, and M. M. Pinter, "Evidence for a spinal central pattern generator in humans a," *Annals of the New York Academy of Sciences*, vol. 860, no. 1, pp. 360–376, 1998.

[34] V. Dietz, "Do human bipeds use quadrupedal coordination?" *Trends in neurosciences*, vol. 25, no. 9, pp. 462–467, 2002.

[35] E. P. Zehr, T. J. Carroll, R. Chua, D. F. Collins, A. Frigon, C. Haridas, S. R. Hundza, and A. K. Thompson, "Possible contributions of cpg activity to the control of rhythmic human arm movement," *Canadian journal of physiology and pharmacology*, vol. 82, no. 8-9, pp. 556–568, 2004.

[36] E. P. Zehr and J. Duysens, "Regulation of arm and leg movement during human locomotion," *The Neuroscientist*, vol. 10, no. 4, pp. 347–361, 2004.

[37] E. R. Kandel, J. H. Schwartz, T. M. Jessell, D. of Biochemistry, M. B. T. Jessell,

S. Siegelbaum, and A. Hudspeth, *Principles of neural science*. McGraw-hill New York, 2000, vol. 4.

[38] C. S. Sherrington, "Flexion-reflex of the limb, crossed extension-reflex, and reflex stepping and standing," *The Journal of physiology*, vol. 40, no. 1-2, pp. 28–121, 1910.

[39] T. G. Brown, "The intrinsic factors in the act of progression in the mammal," *Proceedings of the Royal Society of London. Series B, containing papers of a biological character*, vol. 84, no. 572, pp. 308–319, 1911.

[40] M. L. Shik, "Control of walking and running by means of electrical stimulation of the midbrain," *Biophysics*, vol. 11, pp. 659–666, 1966.

[41] J. Duysens and H. W. Van de Crommert, "Neural control of locomotion; part 1: The central pattern generator from cats to humans," *Gait & posture*, vol. 7, no. 2, pp. 131–141, 1998.

[42] S. P. Swinnen, "Intermanual coordination: from behavioural principles to neural-network interactions," *Nature Reviews Neuroscience*, vol. 3, no. 5, pp. 348–359, 2002.

[43] N. Kawashima, D. Nozaki, M. O. Abe, M. Akai, and K. Nakazawa, "Alternate leg movement amplifies locomotor-like muscle activity in spinal cord injured persons," *Journal of neurophysiology*, vol. 93, no. 2, pp. 777–785, 2005.

[44] V. Dietz and J. Michel, "Human bipeds use quadrupedal coordination during locomotion," *Annals of the New York Academy of Sciences*, vol. 1164, no. 1, pp. 97–103, 2009.

[45] O. White, Y. Bleyenheuft, R. Ronsse, A. M. Smith, J.-L. Thonnard, and P. Lefevre, "Altered gravity highlights central pattern generator mechanisms," *Journal of neurophysiology*, vol. 100, no. 5, pp. 2819–2824, 2008.

[46] P. HOFFMANN, "Beitrage zur kenntnis der menschlichen reflex emit besonderer berucksichtigung der elektrichen. erscheinnungen," *Arch-Physol*, 1910.

[47] E. Bizzi, F. A. Mussa-Ivaldi, and S. Giszter, "Computations underlying the execution of movement: a biological perspective," *Science*, vol. 253, no. 5017, pp. 287–291, 1991.

[48] E. Bizzi, V. Cheung, A. d'Avella, P. Saltiel, and M. Tresch, "Combining modules for movement," *Brain research reviews*, vol. 57, no. 1, pp. 125–133, 2008.

[49] S. F. Giszter, F. A. Mussa-Ivaldi, and E. Bizzi, "Convergent force fields organized in the frog's spinal cord," *Journal of neuroscience*, vol. 13, no. 2, pp. 467–491, 1993.

[50] S. Degallier and A. Ijspeert, "Modeling discrete and rhythmic movements through mo-

tor primitives: a review," *Biological cybernetics*, vol. 103, no. 4, pp. 319–338, 2010.

[51] P. Saltiel, M. C. Tresch, and E. Bizzi, "Spinal cord modular organization and rhythm generation: an nmda iontophoretic study in the frog," *Journal of neurophysiology*, vol. 80, no. 5, pp. 2323–2339, 1998.

[52] P. Saltiel, K. Wyler-Duda, A. d'Avella, R. J. Ajemian, and E. Bizzi, "Localization and connectivity in spinal interneuronal networks: The adduction–caudal extension–flexion rhythm in the frog," *Journal of neurophysiology*, vol. 94, no. 3, pp. 2120–2138, 2005.

[53] J. Kelso, "On the oscillatory basis of movement," in *Bulletin of the psychonomic society*, vol. 18, no. 2. PSYCHONOMIC SOC INC 1710 FORTVIEW RD, AUSTIN, TX 78704, 1981, pp. 63–63.

[54] D. Sternad, "Towards a unified theory of rhythmic and discrete movements—behavioral, modeling and imaging results," in *Coordination: Neural, behavioral and social dynamics*. Springer, 2008, pp. 105–133.

[55] D. Goodman and J. Kelso, "Exploring the functional significance of physiological tremor: a biospectroscopic approach," *Experimental Brain Research*, vol. 49, no. 3, pp. 419–431, 1983.

[56] S. Grossberg, C. Pribe, and M. A. Cohen, "Neural control of interlimb oscillations," *Biological cybernetics*, vol. 77, no. 2, pp. 131–140, 1997.

[57] K. Matsuoka, "Sustained oscillations generated by mutually inhibiting neurons with adaptation," *Biological cybernetics*, vol. 52, no. 6, pp. 367–376, 1985.

[58] ——, "Mechanisms of frequency and pattern control in the neural rhythm generators," *Biological cybernetics*, vol. 56, no. 5-6, pp. 345–353, 1987.

[59] H. Nagashino and J. Kelso, "Bifurcation of oscillatory solutions in a neural oscillator network model for phase transitions," in *Proceedings of the 2nd Symposium on Nonlinear Theory and Its Applications*. Research Society of Nonlinear Theory and Its Applications, IEICE NP, 1991, pp. 119–122.

[60] H. Nagashino and J. S. Kelso, "Phase transitions in oscillatory neural networks," in *Science of artificial neural networks*, vol. 1710. International Society for Optics and Photonics, 1992, pp. 279–287.

[61] H. R. Wilson, "Spikes, decisions, and actions: the dynamical foundations of neurosciences," 1999.

[62] D. V. Vavoulis, V. A. Straub, I. Kemenes, G. Kemenes, J. Feng, and P. R. Benjamin,

"Dynamic control of a central pattern generator circuit: a computational model of the snail feeding network," *European Journal of Neuroscience*, vol. 25, no. 9, pp. 2805–2818, 2007.

[63] A. J. Ijspeert, A. Crespi, D. Ryczko, and J.-M. Cabelguen, "From swimming to walking with a salamander robot driven by a spinal cord model," *science*, vol. 315, no. 5817, pp. 1416–1420, 2007.

[64] D. M. Wolpert, R. C. Miall, and M. Kawato, "Internal models in the cerebellum," *Trends in cognitive sciences*, vol. 2, no. 9, pp. 338–347, 1998.

[65] D. M. Wolpert and Z. Ghahramani, "Computational principles of movement neuroscience," *Nature neuroscience*, vol. 3, no. 11, pp. 1212–1217, 2000.

[66] T. Flash and N. Hogan, "The coordination of arm movements: an experimentally confirmed mathematical model," *Journal of neuroscience*, vol. 5, no. 7, pp. 1688–1703, 1985.

[67] D. Sternad, W. J. Dean, and S. Schaal, "Interaction of rhythmic and discrete pattern generators in single-joint movements," *Human Movement Science*, vol. 19, no. 4, pp. 627–664, 2000.

[68] A. de Rugy, K. Wei, H. Müller, and D. Sternad, "Actively tracking 'passive'stability in a ball bouncing task," *Brain research*, vol. 982, no. 1, pp. 64–78, 2003.

[69] K. Wei, T. M. Dijkstra, and D. Sternad, "Passive stability and active control in a rhythmic task," *Journal of Neurophysiology*, vol. 98, no. 5, pp. 2633–2646, 2007.

[70] R. Ronsse, P. Lefèvre, and R. Sepulchre, "Robotics and neuroscience: A rhythmic interaction," *Neural networks*, vol. 21, no. 4, pp. 577–583, 2008.

[71] H. W. Van de Crommert, T. Mulder, and J. Duysens, "Neural control of locomotion: sensory control of the central pattern generator and its relation to treadmill training," *Gait & posture*, vol. 7, no. 3, pp. 251–263, 1998.

[72] R. Marteniuk, C. MacKenzie, and D. Baba, "Bimanual movement control: Information processing and interaction effects," *The Quarterly Journal of Experimental Psychology Section A*, vol. 36, no. 2, pp. 335–365, 1984.

[73] K. R. Lohse, D. E. Sherwood, and A. F. Healy, "Neuromuscular effects of shifting the focus of attention in a simple force production task," *Journal of Motor Behavior*, vol. 43, no. 2, pp. 173–184, 2011.

[74] S. Grillner, "Locomotion in vertebrates: central mechanisms and reflex interaction," *Physiological reviews*, vol. 55, no. 2, pp. 247–304, 1975.

[75] S. Grillner and P. Wallen, "Central pattern generators for locomotion, with special reference to vertebrates," *Annual review of neuroscience*, vol. 8, no. 1, pp. 233–261, 1985.

[76] D. K. Rose and C. J. Winstein, "Bimanual training after stroke: are two hands better than one?" *Topics in stroke rehabilitation*, vol. 11, no. 4, pp. 20–30, 2004.

[77] H. Heuer, T. Kleinsorge, W. Spijkers, and C. Steglich, "Static and phasic cross-talk effects in discrete bimanual reversal movements," *Journal of Motor Behavior*, vol. 33, no. 1, pp. 67–85, 2001.

Vita

Marcelline E. Dechenaud was born in Saint-Quentin (02), France in 1994. She received the Master grade certificate in mechanical engineering from Polytechnic Universitary School of Lyon 1 University (France) in 2017. Since 2018, she has been Research Assistant in the department of Mathematics at Louisiana State University and Pennington Biomedical Research Center working on developing a software for automated digital anthropometric measurements based on 3D scans. She has also co-founded a company that seeks to overcome the need for uniformity and sharing of clinical data and consequent health prediction models by developing a web application that allows researchers to write publications by gathering data and running appropriate analysis on those pooled data. Early in her educational journey, Marcelline has shown interests in Biomechanics, particularly in the fields of prosthetics in which she wishes to work upon completion of her master's degree in August 2020.